UPPSALA
UNIVERSITET

UPTEC W 21011
Examensarbete 30 hp
Mars 2021

How design storms with normally distributed intensities customized from precipitation radar data in Sweden affect the modeled hydraulic response to extreme rainfalls

Daniel Elfström
Max Stefansson

Abstract

How design storms with normally distributed intensities customized from precipitation radar data in Sweden affect the modeled hydraulic response to extreme rainfalls

Daniel Elfström and Max Stefansson

Intense but short-term cloudbursts may cause severe flooding in urban areas. Such short-term cloudbursts mostly are of convective character, where the rain intensity may vary considerably within relatively small areas. Using uniform design rains where maximum intensity is assumed over the whole catchment is common practice in Sweden, though. This risks overestimating the hydraulic responses, and hence lead to overdimensioning of stormwater systems.

The objective of this study was to determine how the hydraulic response to cloudbursts is affected by the spatial variation of the rain in relation to the catchment size, aiming to enable improved cloudburst mapping in Sweden.
Initially, the spatial variation of heavy rains in Sweden was investigated by studying radar data provided by SMHI. The distribution of rainfall accumulated over two hours from heavy raincells was investigated, based on the assumption that the intensity of convective raincells can be approximated as spatially Gaussian distributed. Based on the results, three Gaussian test rains, whose spatial variation was deemed a representative selection of the radar study, were created.

In order to investigate how the hydraulic peak responses differed between the Gaussian test rains and uniform reference rains, both test and reference rains were modeled in MIKE 21 Flow model. The modelling was performed on an idealised urban model fitted to Swedish urban conditions, consisting of four nested square catchments of different sizes. The investigated hydraulic peak responses were maximum outflow, proportion flooded area and average maximum water depth.

In comparison with spatially varied Gaussian rains centered at the outlets, the uniform design rain with maximum rain volume overestimated the peak hydraulic response with 1-8 %, independent of catchment size. Uniform design rains scaled with an area reduction factor (ARF), which is averaging the rainfall of the Gaussian rain over the catchment, instead underestimated the peak response, in comparison with the Gaussian rains. The underestimation of ARF-rains increased heavily with catchment size, from less than 5 % for a catchment area of 4 km^2 to 13 - 69 % for a catchment area of 36 km^2.

The conclusion can be drawn that catchment size ceases to affect the hydraulic peak response when the time it takes for the whole catchment to contribute to the peak response exceeds the time it takes for the peak to be reached. How much the rain varies over the area which is able to contribute to the peak response during the rain event, can be assumed to decide how much a design rain without ARF overestimates the peak responses. If the catchment exceeds this size, an ARF-scaled rain will underestimate the peak responses. This underestimation is amplified with larger catchments. The strong pointiness of the CDS-hyetograph used in the study risks underestimating the differences in hydraulic peak responses between the test rains and a uniform rain without ARF, while the difference between test rains and uniform rains with ARF risks being overestimated.

Keywords: Cloudbursts, cloudburst mapping, spatial rain variation, pluvial flooding, hydraulic response, Swedish precipitation radar data, idealized urban catchment, hydrodynamic modeling

Department of Earth Sciences, Program for Air, Water and Landscape Sciences, Uppsala University, Villavägen 16, 75236 Uppsala, Sweden.

Referat

How design storms with normally distributed intensities customized from precipitation radar data in Sweden affect the modeled hydraulic response to extreme rainfalls

Daniel Elfström och Max Stefansson

Intensiva men kortvariga skyfall kan orsaka omfattande översvämningsproblematik i urbana områden. Trots att sådana kortvariga skyfall oftast är av konvektiv karaktär, där regnintensiteten kan variera avsevärt inom relativt små områden, används idag uniforma designregn där maxintensitet antas över hela avrinningsområdet. Detta riskerar att leda till en överskattning av hydrauliska responser, och följaktligen överdimensionering av dagvattensystem.

Denna studie syftar till att utreda hur den hydrauliska responsen av skyfall påverkas av regnets spatiala variation, i relation till avrinningsområdets storlek. Ytterst handlar det om att möjliggöra förbättrad skyfallskartering i Sverige.

Initialt undersöktes den spatiala variationen hos kraftiga regn i Sverige, genom en studie av radardata tillhandahållen av SMHI. Utbredningen av regnmängd ackumulerad över två timmar från kraftiga regnceller undersöktes utifrån antagandet att intensiteten hos konvektiva regnceller kan approximeras som spatialt gaussfördelad. Baserat på resultatet skapades tre gaussfördelade testregn vars spatiala variation ansågs utgöra ett representativt urval från radarstudien.

För att undersöka hur de hydrauliska responserna skiljer sig åt mellan de gaussfördelade testregnen och uniforma referensregn, modellerades såväl test- som referensregn i MIKE 21 Flow model. Modelleringen utfördes på en idealiserad stadsmodell anpassad efter svenska urbana förhållanden, bestående av fyra nästlade kvadratiska avrinningsområden av olika storlekar. De hydrauliska responser som undersöktes var maximalt utflöde, maximal andel översvämmad yta samt medelvärdesbildat maximalvattendjup, alltså toppresponser.

Jämfört med spatialt varierade gaussregn centrerade kring utloppen överskattade ett uniformt designregn med testregnens maximala volym de hydrauliska toppresponserna med 1-8 %, oberoende av avrinningsområdets storlek. Uniforma designregn *skalade med area reduction factor* (ARF), vilken medelvärdesbildar gaussregnets nederbörd över avrinningsområdet, underskattade istället toppresponsen jämfört med gaussregnen. ARF-regnets underskattning ökade kraftigt med avrinningsområdets storlek, från mindre än 5 % för ett avrinningsområde på 4 km^2, till 13 - 69 % för ett avrinningsområde på 36 km^2.

Slutsatsen kan dras att avrinningsområdets storlek upphör att påverka den hydrauliska toppresponsen, då tiden det tar för hela avrinningsområdet att samverka till toppresponsen överstiger tiden till denna respons. Hur mycket regnet varierar över det område som under regnhändelsen hinner samverka till toppresponsen, kan antas avgöra hur mycket ett designregn utan ARF överskattar toppresponserna. Överstiger avrinningsområdet denna storlek kommer ett ARF-regn att underskatta toppresponserna, och underskattningen förstärks med ökande avrinningsområdesstorlek. Den kraftiga temporala toppigheten hos den CDS-hyetograf som användes i studien riskerar att underskatta skillnaderna i hydraulisk topprespons mellan testregnen och ett uniformt regn utan ARF, medan skillnaden mellan testregn och uniforma regn med ARF istället riskerar att överskattas.

Nyckelord: Skyfall, skyfallskartering, gaussisk regnfördelning, spatial regnvariation, pluvial översvämning, hydraulisk respons, svensk nederbördsradardata, idealiserat urbant avrinningsområde, hydrodynamisk modellering.

Institutionen för geovetenskaper, Luft- vatten- och landskapslära,
Uppsala Universitet, Villavägen 16, 75236 Uppsala, Sverige.

Preface

This study is a master thesis of 30 credits in the Master Program in Environmental and Water Engineering at Uppsala University and the Swedish University of Agricultural Science, cowritten by Max Stefansson and Daniel Elfström. It has been conducted in collaboration with Tyréns AB and SMHI. Johan Kjellin has been supervising, with help of Jimmy Olsson, both at Tyréns. Gabriele Messori has been subject reader and Erik Sahlée examiner, both at the Department of Earth Sciences, Program for Air, Water and Landscape Sciences, Uppsala University.

We would like to direct a special thanks to Johan Kjellin, for your commitment and interesting input, and to Jimmy Olsson, for your inputs and your indispensable help with MIKE and MATLAB. Also, we would like to thank Jonas Olsson, Peter Berg and Lennart Simonsson at SMHI for providing radar data and interesting input.

Populärvetenskaplig sammanfattning

Kraftiga kortvariga skyfall kan leda till översvämningar i städer. Det beror på att städer, till skillnad från natur, till stor del utgörs av gator, byggnader och andra hårdgjorda ytor som inte kan absorbera regnvattnet. Städer är därför försedda med dagvattensystem för att ta hand om ytavrinningen med hjälp av brunnar och ledningar. Regnar det tillräckligt mycket på kort tid klarar dock inte dagvattensystemet av att sluka allt regnvatten, och översvämningar kan då uppstå i låglänta områden. För att kunna förhindra att vatten blir stående på kritiska platser, exempelvis utanför sjukhus och annan samhällsviktig infrastruktur, utförs så kallad skyfallskartering. I en skyfallskartering undersöks vilka områden som blir översvämmade i händelse av ett svårt skyfall. Skyfallskarteringen utförs i ett modelleringsprogram genom att simulera hur vattnet rinner i en digital modell av staden. I simuleringen tillför man ett regn vars intensitet och mängd är baserad på statistik över extremnederbörd - ett så kallat designregn.

De designregn som används vid skyfallskartering i Sverige idag ansätts lika med den förmodade maxintensiteten över hela staden, medan kraftiga skyfall i själva verket kan variera kraftigt inom ganska små områden. Den extrema korttidsnederbörden i Sverige är nästan uteslutande av konvektiv karaktär - alltså av den typ som ger häftiga regnskurar, ofta med åska, under sommarmånaderna. Som bekant kan sådana regn- och åskskurar vara mycket lokala, och regnmängden kan skilja mycket mellan två närliggande platser. Alltså kan man inte räkna med att den maximala regnmängden faller över något större område. Detta är dock det antagande som görs när man använder ett designregn som inte tar hänsyn till regnets variation över marken, och det kan leda till att risken för översvämning överskattas, vilket i sin tur kan leda till att onödigt dyra åtgärder sätts in för att förhindra översvämningen. Denna studie syftar till att undersöka hur översvämningarna påverkas av den spatiala variationen hos extrema regnskurar.

Intensiteten hos individuella konvektiva regnskurar kan antas vara i princip normalfördelad över marken, från en toppintensitet i skurens mitt. Regnintensiteten kan alltså förenklat visualiseras som en normalfördelad eller gaussformad “puckel” eller “klocka” över marken. Sett uppifrån antas denna “gaussklocka” vara ellipsformad, och kan beskrivas av en standardavvikelse i ellipsens stor- och lillaxel. Om regnmängden ackumuleras över tid medan regnmolnet rör sig, kan den sammanlagda regnmängden på marken likaså approximeras som en ellipsformad gaussklocka - motsvarande ett “fotavtryck” från regnskuren. Utifrån detta antagande analyserades radardata från SMHI av extrema regnhändelser. Nederbörden som mätts upp av radarn ackumulerades över perioder av två timmar, vilket visualiserades som kartor över den totala regnmängd som fallit under den tiden. Ellipser anpassades därefter till fotavtrycken av nederbördsrika regnskurar, och utifrån dessa erhölls statistik över storleken hos de ackumulerade regnskurarna. Med utgångspunkt i resultatet skapades tre gaussformade testregn, vars storlek utgjorde ett representativt urval från de verkliga ackumulerade skurarna.

Därefter skapades en förenklad modell av en typisk svensk stad, genom att sätta samman 400 gånger 400 meter stora likformiga kvartersblock till en 8 gånger 8 km stor modellstad. Varje kvartersblock innehöll gator, torg, grönytor och byggnader, med olika delar som skulle representera stadskärnor, handels-, industri-, lägenhets- och villa- samt naturområden. I programmet MIKE simulerades därefter de gaussformade testregnen med olika

placering i modellstaden, samt designregn med samma regnmängd överallt över staden. Därefter jämfördes de simulerade översvämningarna av gaussregn och designregn i modellen. Översvämningarna skattades genom att mäta maximalt utflöde, maximal andel översvämmad yta, samt medelvärdet av det maximala vattendjupet i varje pixel. Det var alltså enbart maximala responser - toppresponser, som mättes, eftersom det framför allt är dessa som är av intresse vid skyfallskartering.

Det visade sig att ett designregn med de gaussformade testregnens maxintensitet över hela ytan överskattade toppresponserna med mellan 1 och 8 %, i jämförelse med testregnen. Ett designregn med samma medelnederbörd som testregnen överallt underskattade istället översvämningen. Denna underskattning ökade med avrinningsområdets storlek - alltså storleken på området uppströms den del av modellen där responserna mättes. Slutsatsen är att toppresponserna enbart påverkas av det regn som faller inom den del av avrinningsområdet som hinner bidra med vatten innan regnet upphör. För regn med två timmars varaktighet, som testades här, är detta område knappast större än några få kvadratkilometer. Regn som faller längre bort från en punkt än så hinner inte rinna till denna punkt innan den lokala avrinningen till punkten i fråga hunnit avta. Om regnet inte varierar inom det område som kan bidra till toppresponsen kommer den spatiala variationen hos regnet inte spela någon roll för denna respons. I studien verkar testregnen endast ha varierat lite över detta område, och därför blev skillnaderna små mellan de gaussformade testregnen och designregnen med dessas maxintensitet överallt.

Studien hade en del osäkerheter. Bland annat bestod radardatan som användes som utgångspunkt för testregnen av pixlar på 2 gånger 2 km, och den missade därmed hur regnet varierade över mindre områden än så. För att verifiera resultatet skulle radardata med högre upplösning därför behöva undersökas.

Contents

1 Introduction

Cloudbursts, where large amounts of rain falls during a short period of time, causes major problems in urban areas, since these areas typically have high proportions of hardened surfaces which obstruct the infiltration of rainwater. Such extreme short-term rainfalls cause so called *pluvial flooding*, when the stormwater system cannot handle the amount of water. In recent time, Swedish cities have been affected by several severe flooding events, for example in Malmö 2014 and Uppsala 2018 (Hernebring et al., 2015; Leijonhufvud, 2018). Therefore, it is of high importance to dimension the stormwater systems, so that the problems can be prevented in a cost effective way.

In order to investigate the impacts of severe flooding in a city, hydraulic modelling is often performed, for example in cloudburst mapping. By inserting a design rain onto a model of the city, the flooding consequences on the ground - the *hydraulic responses* - are investigated. The design rains gives a certain amount of rain during a certain amount of time, and is based on statistics of the intensity and frequency of real rain events. For cloudburst mapping, the extreme hydraulic responses are of interest, and therefore a very extreme design rain is used, normally based on rain intensities statistically occurring once in 100 years.

The most extreme short-term rainfall in Sweden usually occurs in convective raincells, caused by heating of the ground (Dahlström, 2010). Though such convective raincells often have very limited spatial extent (SMHI, 2017), and the precipitation hence varies over small areas, the design storms used in cloudburst mapping when dimensioning the stormwater systems, are assumed to be spatially uniform. This risks giving misleading results, since the spatial variation of cloudbursts affects the hydraulic response (Adams et al, 1986). Spatially uniform design rains risk overestimating the hydraulic responses, leading to oversized stormwater systems and hence unnecessary costs (Thorndahl et al., 2019).

Several studies (Sharon, 1972; Zawadski, 1973; Marshall, 1980; Jinno et al., 1993) have concluded that the intensity of individual convective raincells can be approximated as spatially *normally distributed* - or with a different term - *Gaussian distributed*. This study uses this assumption for testing the hydraulic responses of spatially varied rains, with Gaussian distributed rain amounts over the ground. The hydraulic responses of those rains, referred to as *test rains*, are compared with the responses of spatially uniform rains corresponding to the design rains used today, referred to as *reference rains*. Since the peak flooding parameters - the *hydraulic peak responses* - such as maximum water depth and maximum water flow is crucial for the severeness of a flooding, peak responses is what is investigated in this study.

The hydraulic response in a point is not only dependent on the rain, but also on the area providing it with runoff. This area is called a *catchment*, and its extent is determined by the topography of the terrain. Since the size of the catchment area might affect the hydraulic responses, this study also investigates the importance of catchment size in relation to the spatial variation of the rain, for the flooding consequences on the ground.

1.1 Aim and objectives

The aim of this study is to obtain an improved understanding of how the hydraulic response to extreme rains is affected by the spatial variation of the rain, in order to enable improved cloudburst mapping in Sweden.

The objective is to determine how the hydraulic peak response of a Swedish urban catchment is affected by the spatial variation of extreme rains in relation to the size of the catchment. Hence, the following questions were formulated:

- How does the catchment and raincell size affect the difference between hydraulic response to a spatially varied test rain and a spatially uniform reference rain with the maximum rainfall of the test rain?
- How does the catchment and raincell size affect the difference between hydraulic response to a spatially varied test rain and a spatially uniform reference rain with the mean rainfall of the test rain, corresponding to an ARF-scaling?

1.2 Delimitations

All tested rains were Chicago Design Storm (CDS) design rains with duration of 2 hours. The maximum rainfall in the test rains were set with 100 years return period, based on the formula given by Dahlström (2010). The test rains were based on a fixed area approach, as cumulative Gaussian raincells accumulated over 2 hours. According to the fixed area approach, the rains were fixed in space, and did not move. The Gaussian shape of the raincells is based on the assumption that the intensity of individual convective raincells can be approximated as normally distributed over the ground, as stated by Jinno et al. (1993).

The catchment model used in this study was designed as an idealized representation of Swedish urban catchments, not as a replica of any specific area.

Only peak hydraulic responses were considered in the results.

1.3 Structure of the report

Hereafter follows a general theory section. The methods, results and discussion are split up into two thematic parts - the first part deals with the radar analysis that was performed in order to create the Gaussian test rains, while the second part deals with the hydraulic modelling of the Gaussian test rains and reference rains for different sizes of urban catchments. The results and discussion in the second part is divided into two partitions: The first partition, written by Elfström, deals with comparison of Gaussian test rains with maximum reference rain, in order to answer the first research question. The second partition, written by Stefansson, deals with comparison of Gaussian test rains with mean reference rains, in order to answer the second research question. Thereafter follows a joint general discussion on the second part of the project. The report ends with a brief general concluding section.

2 Theory

2.1 Fluvial and pluvial flooding

Under Swedish conditions, the rain intensity seldom exceeds the infiltration capacity in the ground. Surface runoff is therefore rare in nature and rural areas, as long as the ground is not saturated with water. Hence, most rainfall in rural areas will percolate down into the groundwater, which eventually will be transported through the terrain to the nearest stream. The water flow in streams will react quite fast to rain, though the bulk of the stream water even after rainfall will be old groundwater, which has been pushed out into the stream due to pressure propagation from higher areas, where the rain percolates. Low areas in the terrain might be flooded, but this is normally because the groundwater surface here is rising above the ground (Grip & Rodhe, 1994). A high groundwater surface is connected to large amounts of precipitation over longer periods of time, or snowmelt. This might eventually also lead to high water levels in watercourses, which might become flooded further downstream. This type of flooding is known as *Fluvial*, and can affect both rural and urban areas.

In urban areas, the hydrological mechanisms are very different from those in nature and rural areas. Here, especially in city centers, a large portion of the ground is constituted by buildings and paved ground, which has practically zero infiltration capacity. The runoff is here to a large extent dependent on an artificial structure, constituted by the stormwater system. This is built up by a system of pipes and ditches that lead the runoff to the nearest water body, connected to the ground by man holes. If the intensity of the rain for some time exceeds the capacity of the stormwater system, it will lead to *pluvial* flooding. The pipes will then be full, and the water will accumulate on the ground. Unlike fluvial flooding, the reason behind this will be short term rainfall with extreme intensities, rather than long-lasting rains or snowmelt.

2.2 Extreme precipitation

2.2.1 Precipitation formation and types

Precipitation is formed by wet air which rises and gets cooled down adiabatically. Since cold air can hold less moisture than warm, the moisture will at some point start condensating or deposit as small water droplets or ice crystals, which form clouds. Over midlatitudes, the temperature in the clouds is usually below zero, and both supercooled water droplets and ice crystals will be formed around small particles in the air. Since the saturation vapour pressure over ice is slightly lower than over water, vapour will be transferred by the air from the water droplets to the ice crystals, which eventually will be heavy enough to fall down as snowflakes. If the temperature below the clouds is above zero, the snowflakes will melt into raindrops before they hit the ground (Raab & Vedin, 1995; Hendriks, 2010).

The different mechanisms that cause the rising of air, creates different types of precipitation. *Convective precipitation* is formed due to local heating of the ground, and is often local and intensive. Columns of warm rising air (thermals) form cumulus clouds which might form intense raincells, often developed as thunderstorms. *Orographic precipitation* is formed when air is pushed up as it is transported in over higher ground at

mountain ranges or highland areas. *Cyclonic precipitation* is formed when air rises in a rotating low-pressure system, and *frontal precipitation* forms when different air masses collide, causing the warmer air to be pushed above the colder air (Hendriks, 2010). In reality, those precipitation types often occur as mixed forms. In synoptic scale weather systems at the mid latitudes, cyclonic and frontal precipitation usually appear together. All other types of precipitation can be enhanced by orographic reinforcement, and convective precipitation is often connected to cold fronts. Also embedded in warm fronts, which usually constitute lasting moderate precipitation, convective precipitation cells might occur (Raab & Vedin, 1995).

2.2.2 Swedish conditions

In Sweden, the majority of the annual precipitation is due to frontal or cyclonic precipitation from synoptic scale weather systems, with low pressure systems connected to the polar front, moving in from the west in the westerly wind belt (Johansson & Chen, 2003). Repeated passage of several rains is, together with snowmelt after snowy winters, the main reason for fluvial flooding in Sweden . Extensive heavy rains in Sweden often occur in connection to slow moving fronts (SMHI, 2018). The most extreme daily precipitation in the country is connected to stationary low-pressure systems, especially at the eastern coast, where a continuous transfer of moisture from the ocean is of importance (Dahlström, 2010).

Pluvial flooding though, is connected to the most extreme rain intensity, which occurs in connection with short term convective precipitation (Dahlström, 2010). In Sweden, as well as northern mid latitudes in general, convective precipitation mainly occurs during summer, and short-term rainfall extremes almost exclusively occur during June - August (Olsson et al., 2014). According to Olsson et al. (2014), intense raincells connected to extreme precipitation in Sweden can be categorized into four typical spatial rainfall patterns: Isolated cells, rain bands with cells, discontinuous rain fields with cells and cells embedded in continuous rain fields.

The intensity and frequency of extreme precipitation in Sweden, long term as well as short term, is supposed to increase in the future, due to a warmer climate. The uncertainties are large, but the intensity of rain with a return period of 10 years is expected to increase by around 10 % for durations from 10 minutes to 24 hours (SMHI, 2020).

2.2.3 Properties of convective precipitation

Convective precipitation occurs when the atmosphere is unstable and the temperature decreases with height faster than the dry adiabatic lapse rate. This is common during summer, when there is a strong heating of the ground by the sun. The unstable conditions enhance vertical movement in the air, and the heated air is at some places lifted by its buoyancy, since warm air is lighter than cold. Adiabatic cooling of the rising air eventually leads to condensation of the moist in the air, forming clouds. This releases latent heat, which reinforces the buoyancy of the cloud and further enhances the convection. The most extreme rain intensities are mainly dependent on the effectiveness and strength of the convection (Dahlström, 2010).

The strength of the convection depends mainly on the amount of water vapor in the

air, which is limited by the temperature, since warm air can contain more moisture than cold, and the buoyancy of the clouds, which is determined by the temperature difference between the cloud and the surrounding atmosphere. This temperature difference is dependent on the degree of instability in the atmosphere and the amount of condensation in the cloud. The height of the convective layer, and hence the cloud, is a measurement of the strength of the convection. The vertical movements stop where the rising air meets a warmer layer (Dahlström, 2010; SMHI, 2019). Since the stratosphere above it is highly stable, the convection can reach no further than the tropopause. The convection is inhibited when dry air from the surrounding atmosphere is mixed into the rising air - so called *entrainment*, which has shown to be an important process. The strength of the convection is also affected by the large scale weather situation. Convergent airflow can for example initiate and strengthen the convection (Dahlström, 2010).

Convective raincells are local features, often with a geographical extent no more than a couple of kilometers (Sharon, 1972; SMHI, 2017), even though they often appear in larger clusters. Studies have shown that the spatial intensity pattern of individual convective raincells often is found to be Gaussian-shaped (Sharon, 1972; Zawadski, 1973; Marshall, 1980; Jinno et al., 1993), even though this adoption cannot be made for rain fields as a whole. This means that the intensity in individual raincells often is normally distributed, with a maximum in the middle. In many cases, the cells are elliptic, not circular, forming an elliptic Gaussian bell-shape, considering the rain intensity over the ground.

2.3 Cloudburst resilient cities

Many cities are vulnerable to flooding from cloudbursts since they often have high amounts of paved surfaces which have properties that enable surface runoff, such as low friction for water runoff and little to no infiltration capacity. Another vulnerability of cities is the amount of buildings and infrastructure of high importance. Cities can increase resilience against cloudbursts through well designed stormwater management systems, but also through creating more areas with high infiltration capacity such as parks and green roofs. Another important aspect is placing important buildings and infrastructure where water from cloudbursts will not accumulate and to have sufficient stormwater management to protect them (MSB, 2017).

2.3.1 Cloudburst mapping

To create resilient cities with well designed stormwater management systems it is important to investigate what parts of the urban area that is prone to flooding, and the amounts of water that can accumulate. This knowledge is needed for prioritizing flood preventing measures at certain areas. Cloudburst mapping shows which surfaces get flooded from extreme rainfalls, as well as the water depth and water flows (MSB, 2017).

There are three main methods used for cloudburst mapping, which are mapping of low points, mapping of surface runoff and mapping of surface runoff and stormwater grids. These methods have different complexities where the more complex models require more data and take longer time to carry out (MSB, 2017).

Mapping of low points
The simplest method is mapping of low points. This method does not use a design storm, hence it is not a true cloudburst mapping method. Instead it only uses detailed elevation data adjusted for buildings and takes about a week to carry out. With a Geographic information system (GIS) low points of every size gets filled with water. This is used to identify low points of the terrain and also gives the extent, volume and depth of every lowpoint, as well as the flow paths between these areas (MSB, 2017).

The risk of the flooding shown in mapping of low points cannot be quantified since it is not related to a design storm with a certain volume or return period. Since hydraulics is not integrated in the method, neither flows nor the flooding over time can be studied. With all these limitations and lack of flooding probability, the use of this model is only suited for identifying vulnerable low points (MSB, 2017).

Mapping of surface runoff
This method uses a two dimensional hydraulic simulation to show the extent of flooding, water depth and surface runoff. The mapping fills low areas with water from upstream areas and gives a physically correct description of ground flows. Test storms with different return periods can be used, also dynamic infiltrations from different surfaces and the capacity of the stormwater systems is integrated through reducing a lump sum of the rain volume (MSB, 2017).

This method is useful for design rains with a return period of over 100 years since the impact of the stormwater system is simplified as a lump sum, leading to greater uncertainties when the rain volume is close to the capacity of the stormwater system. Implementing stormwater systems in this way can cause underestimation of flooding downstream main pipes and overestimate flooding in parts situated upstream, when there are parts of the pipe system with a lack of capacity, which usually occurs more downstream than upstream. The method is cost effective, and is suitable for seeing the overall situation of a city's flooding response (MSB, 2017).

Mapping of surface runoff and stormwater system
Similarly to the surface runoff method this method also uses a two dimensional model for surface runoff but now there is also a one dimensional hydraulic model for the stormwater system connected to it. The dynamics of the stormwater system is thereby included, which means pipes can get filled to their capacity and release water at critical points during the simulation, making it more realistic than a lump sum (MSB, 2017).

The high complexity of this method requires good knowledge in modelling. But unlike the other methods it does not have any limitations related to types of rain which can be studied, or the use of the results. The result from the model can be used for all types of consequence analyses, structure plans, surface level action plans and preparedness planning (MSB, 2017).

Required data
Many decisions about what data to put into the hydraulic model needs to be made before carrying out the hydraulic modeling for cloudburst mapping. In order to describe urban conditions well enough, elevation data of 1-5 meters accuracy is needed to prevent the

extent of flooding to not be too smoothed out. The model resolution can never be higher than the resolution of the elevation data. The elevation data also needs to be manually modified to elevate places with buildings and lower places with bridges. Land use data is used in the model to map out the types of surfaces, in order for the model to have correct infiltration capacities and roughness of the surface, which is important for both horizontal and vertical water flows (MSB, 2017).

The data for implementation of stormwater systems into the model varies greatly between methods with or without 1 dimensional modelling of stormwater systems. If the simpler case is used, then rainwater volume will be reduced by an estimation of the capacity of the stormwater system which is often assumed to be the rain volume associated with a cloudburst with a return period of 10 years. But the reduction of this lump amount should only be done on areas connected to the piping (MSB, 2017).

2.4 Design storms

In order to perform cloudburst mapping, the hydraulic model needs rain input. Standardized rains, so called *design storms* is used for this purpose. The design storms are based on rainfall statistics, and often have a characteristic temporal distribution. In Swedish cloudburst mapping, the design storms are assumed uniform over space.

2.4.1 Intensity-duration-frequency functions

The Intensity-duration-frequency (IDF) function gives rainfall intensities as a function of duration and return period. The function can be visualised as curves of different return periods, where intensity is plotted against duration. A rain with a certain return period is statistically expected to occur once during the return period. The given intensity can easily be translated to volume, by multiplying with the duration. The IDF-relationship is a very useful tool for hydraulic dimensioning since it connects intensity of rains with their statistical frequency. The IDFs used in Sweden today, as well as in this study, was calculated by Dahlström (2010).

2.4.2 Area reduction factors

An area reduction factor is a measurement of the ratio of the maximum areal rainfall divided by the maximum point rainfall, over either a fixed area or within a storm. This method is used to scale maximum design rains, which uses point rainfall of a certain return period, over a whole area.

ARFs are traditionally obtained from spatial correlations from recordings of multiple rain gauges or by empirical estimations of the ratio between maximum areal rainfall, which is spatially averaged rain gauge data and point rainfall over a specific duration within a fixed area. But recently ARFs developed from radar data have been the topic of several studies (Durrans et al., 2002; Pavlovic et al., 2016; Thorndahl et al., 2019).

There are two main classes of ARF - the *storm-centred approach* and the *area-centred approach* - not to confuse with the similarly named methods for Gaussian rain representation. The storm-centred approach looks for the maximum rainfall intensity in a given

domain and estimates the ratio between areal and point rainfall for each storm individually. The area-centred approach is used on a fixed location, where the ratio between maximum areal rainfall with a given return period and maximum point rainfall with the same return period is given by the extreme rainfall statistics at this point.

2.4.3 Chicago design storm hyetographs

A hyetograph is a rain intensity curve, which describes how the rainfall is distributed over time. The Chicago design storm (CDS) is a hyetograph used in cloudburst mapping and hydraulic dimensioning in Sweden, fitted to the IDF-curves based on Swedish rain statistics. One CDS is given for every return period and rain duration. It is constructed in such a way that it simulates the design intensity for all durations, from the given, down to a 10-min event. For a rain of 2 hour duration and 100 years return period, as used in this study, the 10 min peak has the intensity of a rain with 100 years return period and 10 min duration, the 20 min centered around the peak corresponds to the rain that falls during a rain with 20 min duration and 100 years return period and so on, see Figure 1. The advantage of this approach is that it simulates several rain durations at the same time. It is probably rather unlikely that all those durations will reach an intensity corresponding to the same return period during the same rain event, though (Watt & Marsalek, 2013). This might lead to an unlikely pointiness of the CDS-hyetograph, since an unlikely large portion of the rain then will fall during a short part of the duration, which may affect the hydraulic responses. Olsson (2019) found that the CDS resulted in an overestimation of maximum flooding depth, compared with empirical hyetographs.

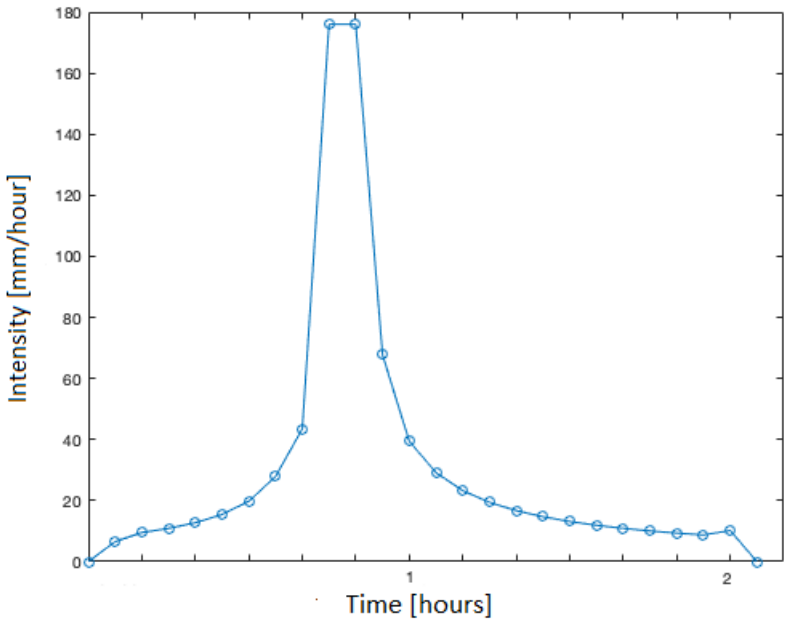

Figure 1: CDS hyetograph with 100 years return period, 2 hour rain duration and 5 min resolution, used as input in this study.

2.5 Sizes of urban catchments in Sweden

Tusher (2019a) used several definitions when investigating the sizes of urban catchments in Sweden. One of those definitions (1b according to Tusher) delimits the catchments

to the urban areas by excluding any rural areas upstream the catchments, and delimited the catchments by rivers and water courses broader than 7 m, according to Lantmäteriet. This definition has been considered relevant for this study, since it deals with pluvial flooding. The contribution from any upstream rural part of the catchment is excluded since it is assumed to be slower than the response of the urban area, and hence not contributing to the peak responses. Rivers wider than 7 m are moreover not expected to propagate a pluvial flooding, since they need a fluvial event in order to flood. According to Tusher (2019a), more than 95 % of the Swedish urban catchments are smaller than 5 km^2, according to the above definition. As seen in Table 1, the very largest urban catchment in the country is, according to the same definition, 33 km^2 large, and only two catchments are larger than 20 km^2, both situated in Stockholm (Tusher, 2019b).

Table 1: The 10 largest urban catchments in Sweden according to criterion 1b in the report by Tusher (2019a). Source: Tusher (2019b).

Catchment size $[km^2]$	**City**
33.2	Stockholm
23.1	Stockholm
17.4	Stockholm
15.0	Stockholm
14.5	Malmö
13.9	Göteborg
12.4	Västerås
12.2	Stockholm
12.1	Stockholm
11.7	Stockholm

2.6 Earlier studies on spatially varied rains

Rainfall is a process with high temporal and spatial heterogeneity, therefore hydrological responses on the catchment-scale are greatly influenced by spatial information of rainfall which can affect the accuracy of hydrological modelling (Singh, 1997). Many researchers, for example Pechlivanidis et al. (2017), have tried to find out "where and when the spatial nature of rainfall is important to runoff response" and the relationship of rainfall and runoff depends on complex relations between rainfall dynamics, physical properties and the spatial scale for a case.

The rainfall-runoff response has been studied in real cases on individual catchments by for example Bell & Moore (2000) and Cole & Moore (2008) but also between catchments with seperate hydrological regimes by Smith et al. (2012). A study of rainfall-runoff response from synthetic rainfall patterns calibrated by real rain data from Mexico City, modelled on synthetic idealised catchments scaled to different sizes by scaling every grid cell, showed peak flows considerably affected by catchment size and spatial variation of rains (Arnaud et al., 2002). Even though the relationship of spatial rainfall and runoff response is the topic of an extensive amount of studies, the conclusions drawn from differ-

ent studies have not always been the same. Many studies have concluded that spatially distributed rainfall is significant for runoff, such as Gabellani et al. (2007) and Patil et al. (2014) and others studies such as Brath et al. (2014) and Lobligeois et al. (2014) concluded that it is not significant. Studies at catchments from different climatic regions on the spatial rainfall–runoff relationship where the spatial and temporal properties of rainfall differ in a significant way has been performed. Some studies focusing on arid and semi-arid regions have described importance of sensitivity of runoff to the spatial and temporal character of the rainfall at different sizes of catchments (Syed et al., 2003). In these climatic regions it was concluded that sensitivity was larger for convective rains compared to frontal events.

The impact of catchment scale has obtained contrasting results, where studies on non urban catchments have shown that with larger catchment scale the significance of spatially varied rains decrease and instead the dominant factor controlling the runoff is catchment response time distribution (Dodov & Foufoula-Georgiou, 2005). Other studies have discussed the role of hillslope and channel travel time on the sensitivity of the hydrological response to rainfall spatial variability (Nicótina et al, 2008; Lobligeois et al., 2014). For some studies which investigated simulated observed runoff-rainfall, the result was that they did not find that scaling catchment areas with spatially varying rain changed the response of runoff.

A recent danish study on ARF:s (Thorndahl et al., 2019) concluded that without regard to the spatial rain variation, uniform design rain would significantly overestimate the rain volume for catchments larger than approximately 10 km^2. The study used 15 years of radar data with 500 m x 500 m resolution from Själland and southwestern Skåne to create estimated storm centric ARF values as functions of area and rain duration. No modelling of the hydraulic responses were performed in the study.

Part 1
Analysis of precipitation radar data

3 Data and methods

3.1 HIPRAD-data

Quality controlled data from the precipitation radar HIPRAD was provided by the Swedish Meteorological and Hydrological Institute (SMHI) from a number of rain events where extreme amounts of rain had been registered during 2 hours in SMHI:s rain gauges during the years 2000 to 2018. The data has a spatial resolution of 2 km x 2 km, and a temporal resolution of 15 minutes. The provided data included radar measurements from a few hours before the event measured by the gauge, until a few hours after it, and it included an area of 200 km x 200 km centered around the gauge. Together with the data itself, a visual representation of the data was provided. This visual representation was in the form of coloured maps for each time step, showing a change of colour at 1, 2, 5, 10, 20 and 50 mm/hour, as recorded by the radar.

3.2 Preliminary visual analysis and data selection

At first, the visual representation of each event where 39 mm or more was recorded by the gauges within 2 hours, corresponding to at least a 20-year rain for a generic place in Sweden (MSB, 2017), was analysed. One of the events was rejected, since the radar showed no precipitation over the gauge. For each of the other events, one or more raincells were analysed (in most cases the cell passing through the gauge, but in several cases other cells with a striking appearance). In total 49 cells from 29 events were analysed. Six more events were analysed, but excluded due to weak observed rain intensity. The chosen cells were approximated as ellipses from the area where the radar was showing the same precipitation intensity as the cell maximum and one degree lower, according to the colour scale. For example, if the cell reached more than 50 mm/h according to the radar, the ellipse was approximately delimited by the extension of the area with at least 20 mm/h according to the radar, and if the cell reached maximum 20-50 mm/h, the ellipse was delimited by the extension of the area with at least 10 mm/h, and so on. According to this simple visual test, the raincells were categorized with respect to size: length and width of the approximated ellipse. Furthermore, the direction of movement for each cell relative to the direction of the major axis of the approximated ellipse was listed, together with their geographical position in Sweden. In addition, the overall precipitation pattern of each event was categorized according to Olsson et al (2013).

Raincells instantaneously measured with the radar are referred to as rain intensity cells.

3.3 Analysis of rain intensity cells

The HIPRAD-data from the 29 chosen events were plotted in Matrix Laboratory (MATLAB), producing maps for each event and time step, showing precipitation intensity with intensity steps of 5 mm/h, enabling a finer analysis of the raincells. As before, the chosen cells were visually approximated as ellipses, whose length and width were listed for

statistical analysis. However, the extent of the ellipse was approximately delimited by the area with more than 61 % of the maximum measured precipitation intensity of the raincell, corresponding to the value one standard deviation away from the center in a Gaussian function, compared to the maximum value in the center, see Figure 2. Thus, the obtained radius of the ellipse would directly approximate the standard deviation of a Gaussian function fitted to the cell.

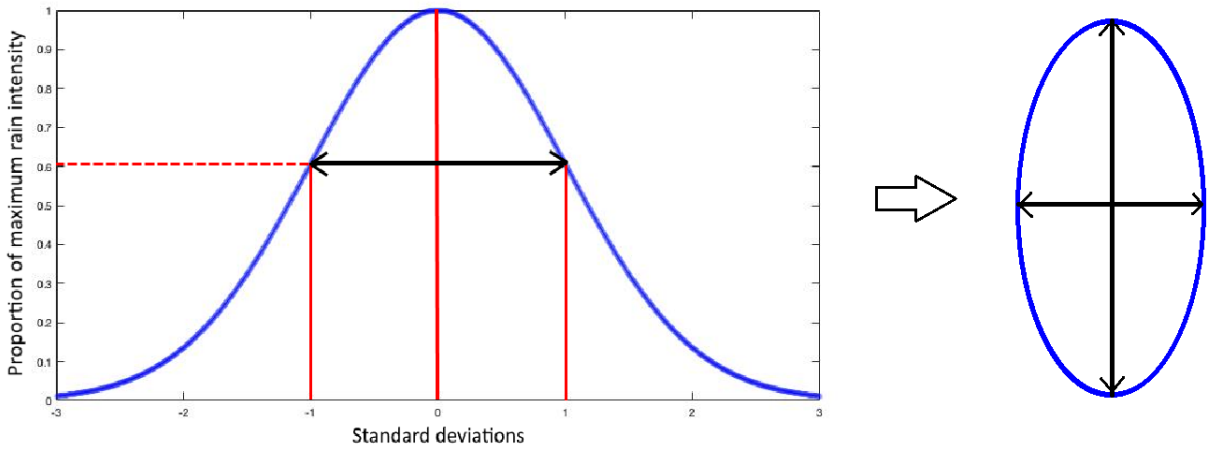

Figure 2: The size of the raincells from the radar data are defined by measuring the size of the parts of the cells holding 61 % or more of the maximum intensity (left). Approximating the intensity of the raincells as spatially Gaussian distributed, this corresponds to the size of an ellipse with semi-major and semi-minor axis corresponding to the standard deviations of the fitted Gaussian shape (right).

The value 61 % is obtained from the probability density function of the Gaussian distribution, *f*. Setting the mean or expectation of the distribution to zero gives the probability density function shown in Equation 1:

$$f(\sigma) = \frac{1}{\sqrt{2\pi}} e^{-\frac{1}{2}\sigma^2} \tag{1}$$

where σ is the standard deviation. Setting σ to one, gives the value of the function one standard deviation away from the maximum value, shown in Equation 2:

$$f(1) = \frac{1}{\sqrt{2\pi}} e^{-1/2} \tag{2}$$

Setting σ to zero gives the maximum value of the function, calculated i Equation 3:

$$f_{max} = f(0) = \frac{1}{\sqrt{2\pi}} e^{-0} = \frac{1}{\sqrt{2\pi}} \tag{3}$$

By multiplying both values by $\sqrt{2\pi}$, the value one standard deviation away from the middle can be described in terms of the the maximum value as shown in Equation 4:

$$e^{-1/2} = 0.607 \approx 61\% \tag{4}$$

Henceforth, the terms *relative width* and *relative length* are used for describing the width and length of the fitted ellipses along the semi-minor and semi-major axis. The relative length and width hence corresponds to double the standard deviations of the intensity in those two directions.

3.4 Analysis of cumulative rainfall cells

With regard to the obtained intensity maps, 2-hour segments were chosen from the 6 hour long time series of each event, as the time periods with most intense precipitation. The radar intensity from the selected 2-hour segments were accumulated in MATLAB, obtaining radar measured rainfall during the 2 hours over the entire radar image area and providing a map with 5 mm steps for each 2-hour rain event. In these maps, 48 cells with large amounts of rainfall were identified, corresponding to earlier analysed intensity cells. As with the intensity cells, these accumulated rainfall cells were approximated as ellipses delimited at 61 % of their maximum rainfall, whose relative length and width were listed for statistical analyses, for an example see Figure 3. Cells reaching less than 15 mm when accumulated were omitted from further analyses. In total, 48 cells from 27 radar events were analysed.

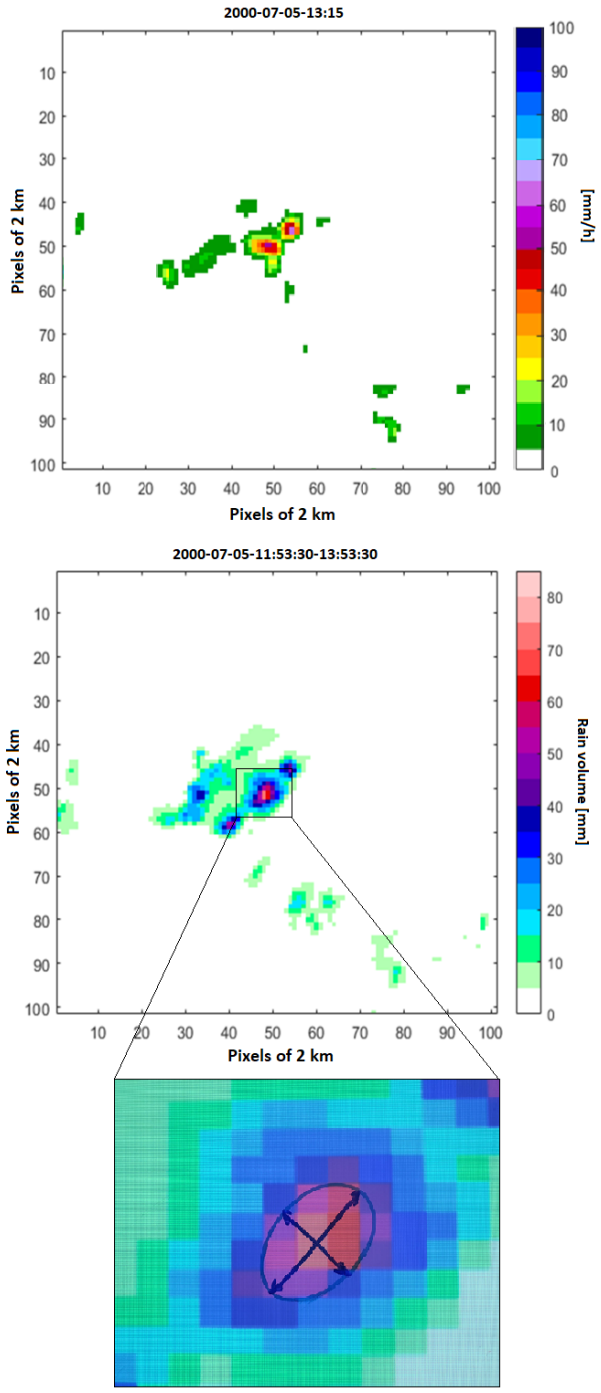

Figure 3: At the top: A map of rain intensities from one time step of one of the analysed HIPRAD events. Middle: A map of the cumulative rain volumes from the same event over the same area, accumulated over 2 h. At the bottom: Zooming in on one of the analysed cumulative raincells from the event, fitted as an ellipse delimited at approximately 61 % of the maximum intensity. This particular cell has a relative width of 5.5 km and a relative length of 9 km.

4 Results

4.1 Rain intensity cells

The results from the radar data analysis of the 44 chosen rain intensity cells are shown in Figure 4 and Tables 2 and 3 below. The relative width and length are defined as twice the size of the standard deviation of the axis of an Gaussian ellipse fitted to the cells, see Figure 2. This spatial standard deviation defining the width and length of the cells is not to be intermixed with the standard deviations shown in the tables, that is a measurement of the statistical distribution of the spatial measurement.

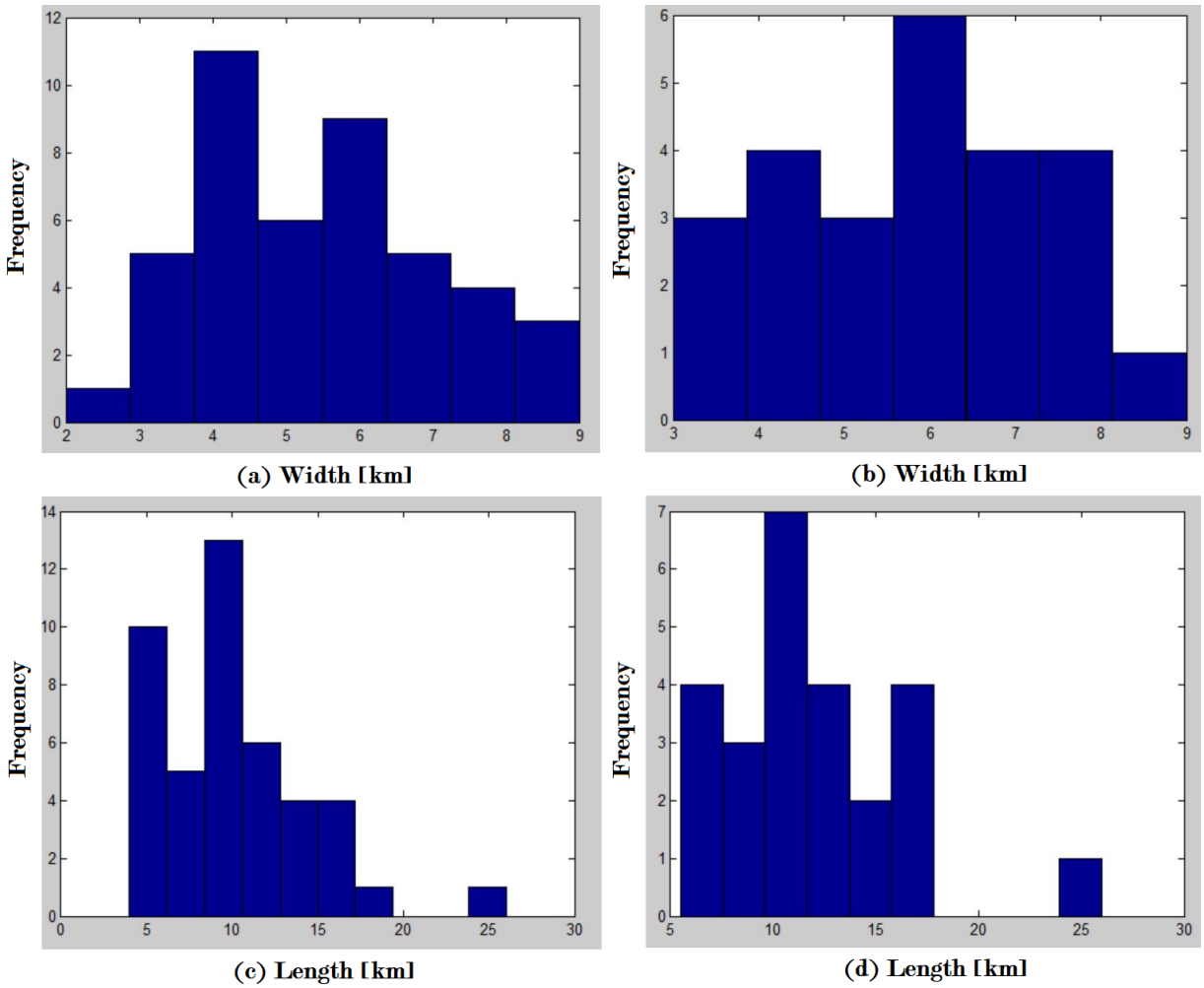

Figure 3: (a): Distribution of the width of every analyzed rain intensity cell. (b): Distribution of the width of the analyzed rain intensity cells which reach 60 mm/h. (c): Distribution of the length of every analyzed rain intensity cell. (d): Distribution of length of the analysed rain intensity cells which reach 60mm/h.

Table 2: Statistical properties of relative length and width of analysed rain intensity cells.

Relative width and length	**Mean**	**Standard deviation**	**Skewness**	**Modal value**
Relative width [km]	5,5	1,7	0,18	4
Relative length [km]	10,1	3,3	1,20	9

Table 3: Relative sizes of rain intensity cells with regard to maximum intensity class

Mean +- standard deviation for rain intensity cells	**All cells**	**Cells with maximum intensity above 60 mm/h**	**Cells with maximum intensity below 60 mm/h**
Relative width [km]	5.5 +- 1.73	5.92 +-1.62	4.95 +-1.74
Relative length [km]	10.13 +- 4.34	11.62 +- 4.39	8.16 +-3.48

As seen in Table 2, the rain intensity cells had a mean relative width of 5.5 km and a mean relative length of 10.1 km. The distributions of both parameters had modal values slightly lower than the means, and show some positive skewness, especially the

relative length. As seen in Table 3, rain intensity cells with a higher measured maximum intensity (over 60 mm/h) tended to be somewhat larger in relative size than cells with lower maximum intensity. Figure 4 shows histograms of the relative width of the rain intensity cells on the upper row, and relative length on the lower row. The histograms to the left show the results for all the analyzed cells, while the histograms to the right show the results for cells with maximum intensity reaching 60 mm/h or more.

Table 4: Ratio of length divided by width for the rain intensity cells.

Length/width ratio	**Mean**	**Standard deviation**
Rain intensity cells	1.88	0.68

The ratio of length divided by width for the rain intensity cells showed to be around 1.9, with a relatively large variation, as seen in Table 4.

4.2 Cumulative rainfall cells

With Cumulative rainfall cells, cells with rain amount accumulated over 2 h from the radar data, is referred. The definitions of relative length and width are the same as for the rain intensity cells, and the same separation needs here to be made between the spatial standard deviation defining the size, and the statistical standard deviation shown in the tables below, as for the rain intensity statistics. 48 cumulative rainfall cells were analysed.

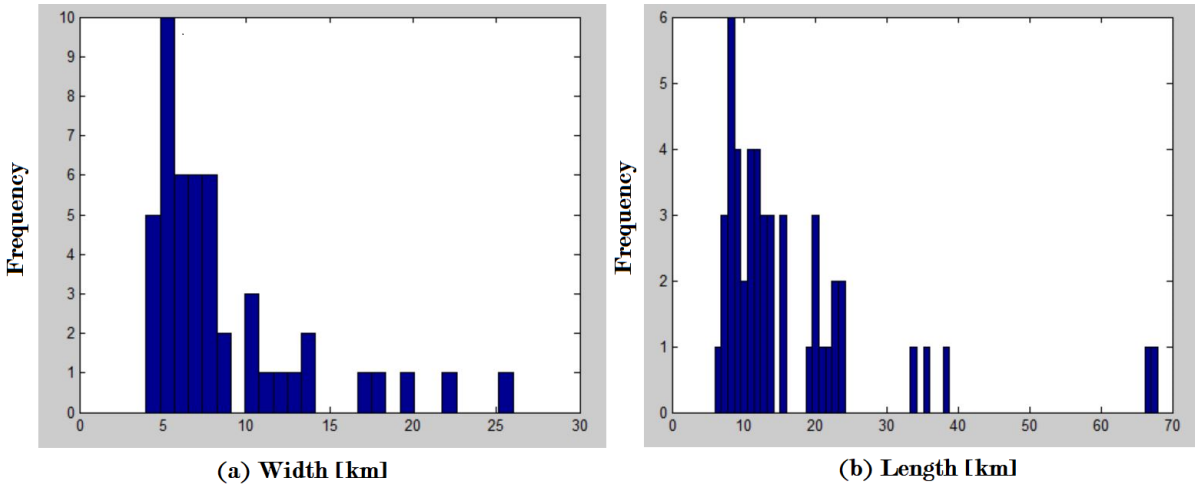

Figure 4: (a): Distribution of relative widths of every analyzed cumulative raincell. (b): Distribution of relative length of every analysed cumulative raincell.

Table 5: Statistical properties of the relative length and width of the cumulative rainfall cells.

Relative width and length of cumulative rainfall cells	**Mean**	**Standard deviation**	**Skewness**	**Modal value**
Relative width [km]	8.6	4.8	1.8	5
Relative length [km]	16.9	13.1	2.6	8 (with coarser resolution 10)

Histograms created from both the relative width and relative length of the ellipses approximated from the cumulative rainfall cells are shown in Figure 5 above. It is clear

to see that they do not show a perfect normal distribution. Both histograms show a large collection of values piling up to the left, while they have long positive tails with larger values. Hence, the distribution of relative size, both length and width, in this case shows strong positive skewness, especially when it comes to the relative width. It is also clear from Table 5 that the mean and modal values of both relative length and width are clearly separated, due to the positive skewness of their distributions. The mean relative width was 8.6 km while the most common relative width was 5 km. When it comes to relative length, the mean is around 17 while the most common length showed to be 8. When regarding the full histogram with rougher resolution though, the modal value ends up somewhere around 10.

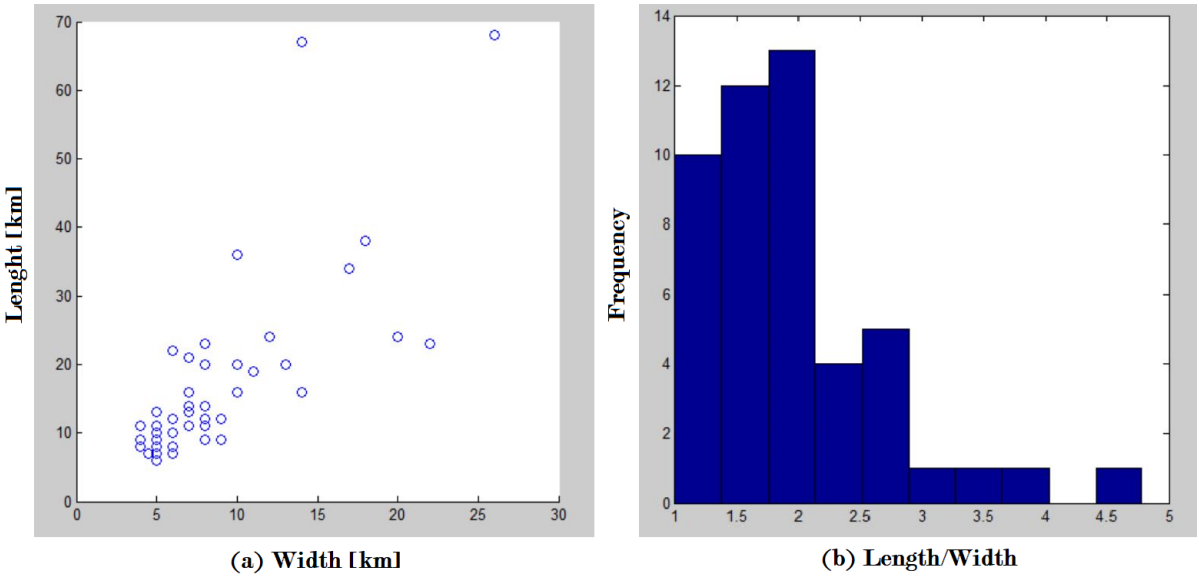

Figure 5: (a): Relative length against relative width for every cumulative raincell. Note that the scale of the y-axis differs from the scale of the x-axis. (b): Distribution of the ratio of relative length/width for every analysed cumulative raincell.

In Figure 6, a scatterplot made with the relative length against relative width of 48 chosen cumulative rainfall cells, is presented together with a histogram of the distribution of length/width ratio from the same ellipses. The scatter plot clearly shows the distribution of cumulative cell sizes. Inspection of the scatterplot shows a cluster of cells with relative width between 4-9 km and relative lengths 4-15 km, where a large portion of the analysed cumulative cells are found. They represent the cluster of relative length and width around the modal value in the histograms of Figure 4. Up to the right of the scatterplot the circles seem to gradually get more and more spread out, while preserving an approximate length-width ratio around 2. The histogram for length/width ratio of the cumulative rain intensity cells shows a modal value around 2, and with a long positive tail.

Table 6: Statistical properties of the relative length and width of the cumulative rainfall cells.

Relative length/width	**Mean**	**Standard deviation**
All cumulative rainfall cells	1.97	0.74
Cumulative rainfall cells with width up to 12 km	1.96	0.62
Cumulative rainfall cells with width up to 8 km	1.97	0.58
Cumulative rainfall cells with width up to 6 km	1.96	0.59

In Table 6, the length/width ratio of the 48 analyzed volume cells are shown. Cells of different widths were analysed separately to see if the length/width ratio differed for cells of different sizes. The results clearly show that the width/length-ratio was independent of cell width.

4.3 Relative cell sizes with regard to spatial rain pattern

The mean relative width and length of cells were calculated for four types of spatial categories made by Olsson et al (2013), for both rain intensity cells and cumulative rainfall cells. The result is presented in Table 7 below. Some events were hard to categorize, and those are omitted from the statistics. Dc (discontinuous fields with cells) was the most common spatial category, while the rest suffer from relatively few examples, (especially category I - individual raincells, with only 3 analysed cells), leading to high uncertainties in the result.

Table 7: *Mean relative length* x *mean relative length* for rain intensity cells and cumulative rainfall cells, with regard to spatial rain pattern. The relative length to width-ratio in parenthesis. Dc: Discontinuous fields with cells. Cc: Continuous fields with cells. B: Rain bands. I: Individual cells. The mean relative length to width ratio is shown in parenthesis.

Spatial rain pattern	**Rain intensity cells**	**Cumulative rainfall cells**
Dc	4.8 x 7.9 km (1.65)	6.4 x 10.6 km (1.65)
Cc	6.3 x 13.6 km (2.16)	12.4 x 32.5 km (2.63)
B	6.4 x 12.5 km (1.97)	8.2 x 15.0 km (1.84)
I	3.5 x 5.7 km (1.62)	5.7 x 8.7 km (1.59)

Regarding rain intensity cells, the categories Cc (continuous fields with cells) and B (rain bands) showed somewhat larger cells, while category I showed smaller cells. Regarding cumulative rainfall cells, the category Cc showed much larger cells, and seems to be responsible for the very large cumulative cells that occur in the overall statistics. The cumulative Cc-cells also shows a higher length to width-ratio than all other cells.

5 Discussion and concluding remarks

5.1 Length to width-ratio of raincells

The average relative length to width-ratio showed to be quite similar for the rain intensity cells and the cumulative rainfall cells, with an average of 1.88 for the intensity cells and 1.97 for the cumulative ones. This is somewhat unexpected, since a relatively stable raincell moving along a straight path would give a more oblong cell when accumulated, and hence the cumulative rainfall cells were expected to have a much higher length to width-ratio than the instantaneous rain intensity cells. Apparently, this was not the case. This implies that the raincells either move very slowly and hardly change position within the two hours of accumulation, or that they change their rain intensity fast in comparison to their movement. Considering the radar sequences from the analysed data, the latter explanation seems to be the main reason. Convective precipitation is a highly dynamic process, and the rain intensity in convective raincells seems to change fast in time according to this study. Hence, the most intense stage of their life cycle does not seem to survive over long distances while advected. An interesting exception seems to be raincells embedded in larger continuous rain fields (classified as Cc in Table 7). These

cells show an average length to width-ratio of 2.6 when accumulated, higher than for the corresponding intensity cells on average, as well as the average for the cumulative cells belonging to the other categories of spatial rain pattern (see Table 7). An explanation could be that the raincells embedded in larger rain fields are maintained by some kind of frontal structure or low pressure system, and hence can uphold high intensity for a longer time while advected.

5.2 Relative sizes with regard to intensity

The intensity cells with maximum intensity exceeding 60 mm/h showed slightly larger relative sizes than those with less intensity. One must consider that the radar intensities were encumbered with uncertainties, as the precipitation measured by the radar often differed from that measured by rain gauges. Even though it is not certain, it seems like the relative size of the raincells slowly increases with intensity. Hence, the relative size of cumulative raincells can be expected to slowly increase with rain volume - and hence increase with the return period of the event. Several studies on area reduction factors (ARF) have found that the ARF:s are decreasing with higher return periods (Skaugen, 1997; Asqiuth & Famiglietti, 2000; Allen & DeGaetano, 2005), while others found no dependence on return period, (Grebner & Roesch, 1997). A smaller storm-centric ARF corresponds to a smaller relative size of the raincell.

5.3 Relative sizes and scenarios of raincells

Regarding relative length and width, the analysed cumulative raincells shows a clear pattern, shown in Figure 7 below, with a large collection of cells piling up relatively close to the smallest sizes, and a wide tail of larger cells gradually spreading out to larger sizes. The bulk of the analysed cumulative raincells seems fairly well gathered around a relative width of 5 km or slightly more, and a length of around 10 km. This coincides quite well with the overall relative size distribution of the rain intensity cells. The modal values of relative width and length for cumulative raincells (5 and 10 km respectively) also coincide well with the average relative width and length for the rain intensity cells (5.5 and 10,1 km respectively), even though the cumulative cells are larger on average, due to the widespread tail of larger cumulative cells. This tells us that the most frequent scenario of the analysed cases with large amounts of precipitation accumulated over 2 hours, seem to be when one raincell passes over a place with its short side first, during its short most intense stage.

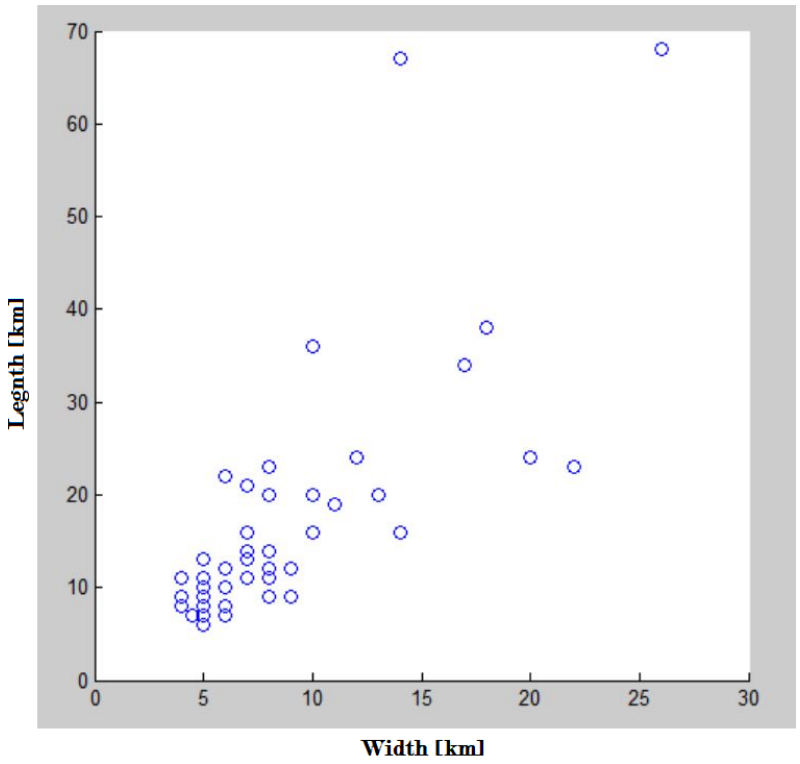

Figure 6: Relative length against relative width for the analysed cumulative raincell. Note that the scale of the y-axis differs from the scale of the x-axis.

In this study, the lower limit of cell sizes is of high interest, since cells with low relative size have the highest spatial variability. The smallest analysed cumulative rainfall cells had a relative size of 4 km, corresponding to 2 pixels of the radar data. Considering the analysed rain intensity cells, there was one cell with width of only 2 km, corresponding to one pixel of the radar data. Hence, the resolution of the radar data (2 km x 2 km) was in this case too coarse to be able to describe the spatial extent of the cell in a proper way. Radar data with finer resolution is requested for further studies. Furthermore, there were no analysed cumulative cells as small as the smallest intensity cells. In theory though, such small cumulative cells - with a width smaller than 4 km - might be possible, in case a very small raincell happens to be very stationary over time, even if it might be unlikely.

Considering the larger cumulative rainfall cells, there can be several explanations for their larger relative width and size. The cells slightly wider than the bulk of values piling up close to the smallest cells might be due to raincells passing with their broadside, or two or more cells passing on slightly different paths, widening the cumulative cells. The largest cumulative cells, with larger relative length and width than any of the non accumulated rain intensity cells, can be distinguished with regard to overall spatial rain pattern, according to the categories made by Olsson et al (2013). They are in most cases raincells embedded in continuous rain fields, and in some cases rain bands with cells (Bc). These large cells are less interesting for this study, since they have smaller spatial variation.

5.4 Uncertainties

This study is encumbered with some uncertainties. Firstly, the resolution of the radar data of 2 km x 2 km is quite coarse. The variation within these grid cells can not be captured by the radar. This complicates the analysis of the small raincells especially, whose intensities can vary strongly over small areas. Data of higher resolution would be of great benefit for future studies. A recent study by Thorndahl et al. (2019) estimated area reduction factors using precipitation radar data from the Öresund region with a resolution of 500 m x 500 m. Using radar data of that resolution would have been beneficial for this study, but it was not available for most of Sweden.

It has not been plausible to analytically test the assumption which the analysis is built upon - namely that the intensity of individual raincells spatially can be approximated with Gaussian functions - partly because of the coarseness of the radar data. An inspection of the visualized radar data though show that the Gaussian approximation seems reasonable for individual raincells as a whole, even though atmospheric convection is a chaotic process, and every raincell has its own characteristics.

Lastly, the method which is used to determine the relative length and width of the raincells, which is built upon visual inspection, might be seen as somewhat subjective. An automatic method might not necessarily have given a more accurate result, but it might have been preferable, since it can be seen as more objective. A possible method would be to fit the ellipses to the raincells in a numerical program, instead of doing it by hand. The general distribution of cell sizes, and the conclusions which can be drawn thereof, would however most likely not have been affected by the subjectivity of the method.

Part 2
Modelling of hydraulic response

6 Model setup and methods

6.1 Gaussian raincell model for test rains

The spatially varied test rains were shaped as elliptic Gaussian cells in terms of the spatial distribution of accumulated rainfall. Three test rains were shaped as 2D-Gaussian functions, with the major axis twice as long as the minor axis, as the mean ratio between the major and minor axis showed to be close to 2, according to the radar data analysis of cumulative raincells. The maximum rainfall was set to 65,2 mm (a rain with 100 years return time for a duration of 2 hours, according to Dahlström (2010)) in the cell center. The rainfall volume was then set to decrease with distance from the cell center, described by a 1D-Gaussian function each for the major- and minor axis of the ellipse describing the form of the cell. These Gaussian functions were described by their standard deviations, defining the spatial variation of rainfall in the model. The following three test rains were chosen as three different sizes of elliptic Gaussian cells, with regard to the statistics of rainfall- and intensity cell sizes obtained from the radar data.

Test rain 1: Elliptic cell with standard deviation of 2 km in the minor axis and 4 km in the major axis. Defining the relative cell size as the spatial extent of rainfall within one standard deviation away from the cell center, this gives a relative size of 4 x 8 km. This corresponds with the approximate relative size of the smallest observed cumulative raincells in the radar analysis, as the smallest observed relative width was 4 km, or 2 pixels. It should represent the smallest cell regarding relative size - and hence, the spatially most varied cumulative raincells that can be expected to occur in Sweden. The smallest (in relative size) and most spatially varied occurring cumulative rainfall cells set the lower limit for how small a catchment area can be and still have a hydraulic response affected by the spatial variation of rain.

Test rain 2: Elliptic raincell with standard deviation of 2.75 km in the minor axis and 5.5 km in the major axis. This gives, according to the above definition, a relative cell size of 5.5 x 11 km. This corresponds approximately with the most common relative size of the observed cumulative raincells, and hence gives an approximation of the most probable relative size of a cumulative raincell that strikes a city. A relative width of 5.5 km corresponds approximately to the 30th percentile according to the radar analysis. In addition, the relative width of this cell is equal to the mean relative width of the noncumulative rain intensity cells according to the radar analysis. Hence, this test rain would correspond to a medium relative sized convective storm cell passing with its short side in front, during its peak temporal intensity. This can be regarded as a probable scenario for a rain event with 2 hours duration and long return period.

Test rain 3: Elliptic cell with standard deviation of 4 km in the minor axis and 8 km in the major axis. This gives, according to the above definition, a relative cell size of 8 x 16 km. This is rather close to the mean relative size of the observed cumulative raincells (8.6 x 16.9 km), and the relative width of 8 km corresponds approximately to

the 60th percentile from the radar analysis. This size also corresponds to the upper limit of the dense lump of sizes around modality. The Cells with the largest relative size are less relevant to use as a test rain, since they give much less spatial variation in rainfall than the smaller ones.

In summary, test rain 1 corresponds to the smallest raincells observed in this study regarding relative width. Test rain 2 corresponds to approximately the 30th percentile regarding relative width, and represents approximately the modal cell size from the study. Test rain 3 corresponds to approximately the 60th percentile regarding relative width, and is close to the mean regarding relative size of the observed raincells.

6.2 Reference rains

As reference rain, spatially uniform rain with 2 hour duration was used. In order to answer the questions of the study objectives, rains with different rain volumes were constructed related to either maximum or mean rain volume of the test rains. This meant the following reference rains:

Maximum reference rain: A spatially uniform reference rain was created with the same maximum cumulative rainfall as in the test rains, 65.2 mm, everywhere. Since the maximum intensity was the same for all test rains and scenarios, only one maximum reference rain was needed.

Mean reference rains: For every simulated scenario, one spatially uniform reference rain was created with the cumulative rain volume set as the spatially mean rain volume of the test rain in the catchment corresponding to the respective scenario.

All test rains and reference rains used Chicago Design Storm (CDS) hyetographs as temporal distribution.

6.3 Urban catchment model

For testing the hydraulic response to the test- and reference rains in MIKE 21 (see section 6.4), a generic model of an urban catchment was constructed in ArcMap. The model was designed as a square catchment with size 8 km x 8 km (in total 64 km^2), with the outlet in one corner, and a main drainage path diagonally through the square, see Figure 8. Nested square subcatchments were constructed in the model, with sizes of 2 km x 2 km, 4 km x 4 km and 6 km x 6 km, giving four catchments of sizes of 4, 16, 36 and 64 km^2 respectively, including the complete model, all with the same square shape. The nested catchments in the urban model is referred to as follows: 2 km x 2 km: A, 4 km x 4 km: B, 6 km x 6 km: C, and the entire model of 8 km x 8 km: D. According to Tusher (2019a), 95 % of all urban catchments in Sweden which are not cut through by major watercourses, are smaller than 5 km^2. The largest urban catchment according to the same definition was 33 km^2, situated in Stockholm (Tusher, 2019b). The catchment model hence represents sizes of Swedish urban catchments with a well taken margin. Using catchment sizes less than 2 km x 2 km was regarded inappropriate, since that was the resolution of the precipitation radar used for constructing the test rains.

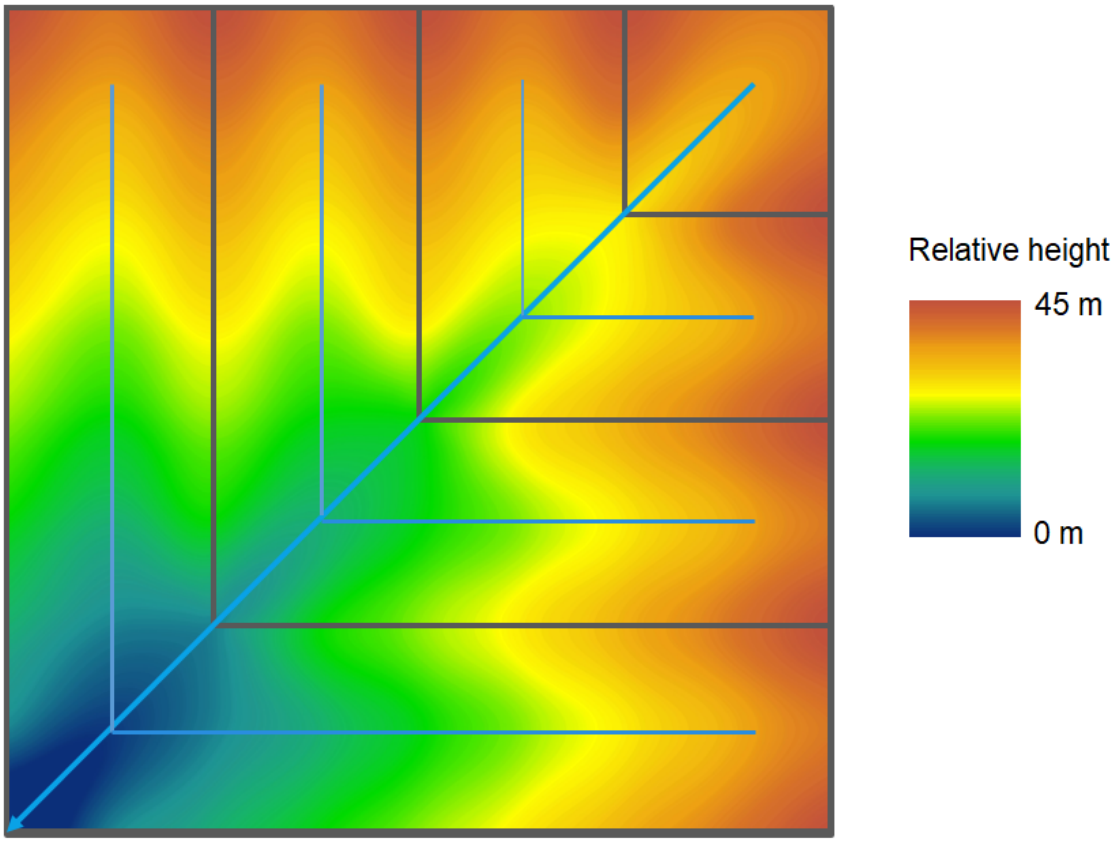

Figure 7: Map showing the general structure and the topography of the urban catchment model. The four nested square catchments of sizes 2 km x 2 km, 4 km x 4 km, 6 km x 6 km and 8 km x 8 km are shown delimited with dark gray lines, where the entire model corresponds to the largest catchment. The principal drainage paths are shown in blue lines, with the main drainage path diagonally through the model. The background colour is showing the topography, with blue colours representing the lowest terrain and red colours representing the highest terrain. The total height difference within the model is set to 45 m.

The topography of the catchment model was set in order to obtain waterflow in accordance with the three nested subcatchments, see Figure 8. The complete topography was created in ArcMap as a spline interpolation between a number of points with defined height. The total relative height difference within the model was set to 45 m, with the lowest point at the outlet, and the highest points where the subcatchment water dividers intersect with the model border. This yielded a slope of 1.4 ‰ along the main drainage path, and 2 ‰ along the auxiliary drainage paths in each subcatchment.

A total relative height difference of 45 m over an area of 64 km^2 is relatively low in comparison to most Swedish cities. It is comparable to the conditions in cities located on clay plains, like Malmö, and to some degree Uppsala. Stockholm and Göteborg are located in joint valley landscapes (*Swedish: sprickdalslandskap*) with somewhat higher relative height differences. Especially the small scale topography in such a landscape is much more pronounced than in the model. The steep slopes that frequently occur in such landscapes are however concentrated to higher terrain with rock and moraine, while the low terrain, where the main water flow paths are located, are constituted by flat valleys with clay, with slopes comparable to those in the model. The model topography was set

in accordance, since the main water flow paths were considered more important than the higher terrain, where less water flows. Hence, the model topography can be considered representative for most larger cities in Sweden, except those located in hilly terrain with higher relative height differences, like Jönköping and Sundsvall.

The urban catchment model was constructed separating between four kinds of features: Impervious surfaces (representing hardened surfaces like pavement and asphalt), pervious surfaces (representing non hardened surfaces like lawns and nature), buildings and low points (low terrain without topographical outlets, in this case pervious). The resolution was set to 10 m, and roads were built one grid wide. This is a rather coarse resolution, but since the aim of the study is not where water flows in a high detail manor but rather the hydraulic responses over larger areas, the correct direction of water flow on a larger scale is sufficient.

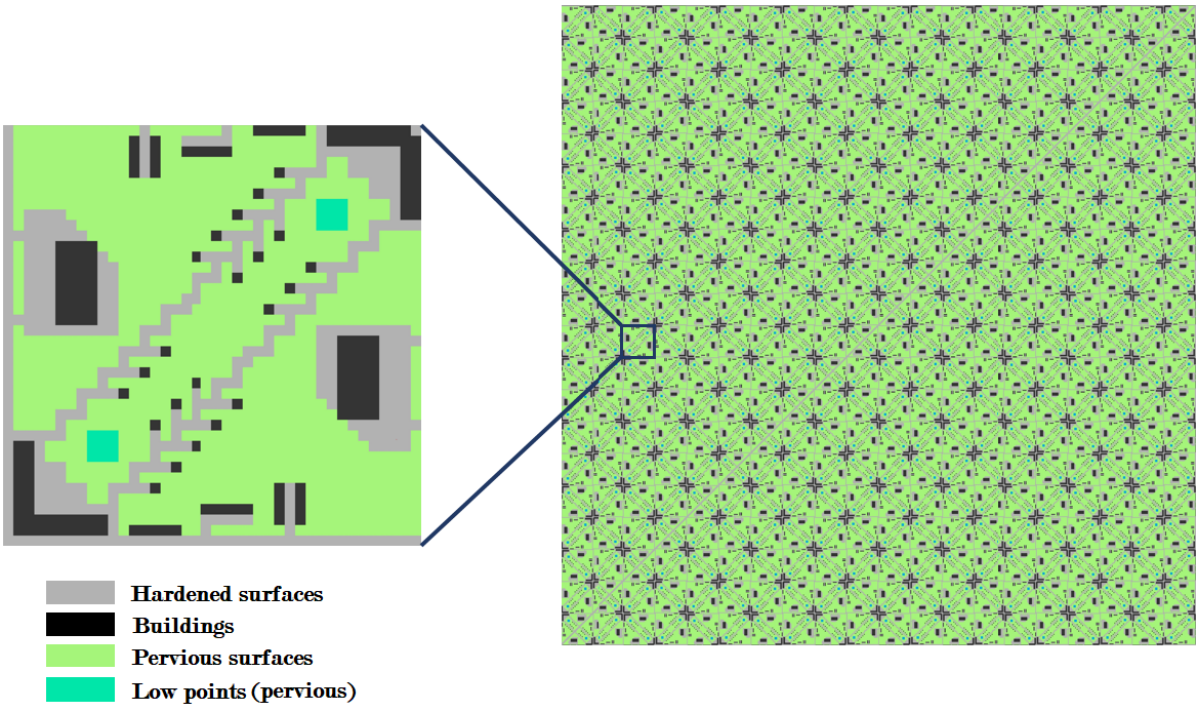

Figure 8: Illustration showing how the entire urban catchment model, to the right, is constructed by arrangements of uniform blocks of 400 m x 400 m, shown to the left. An unobstructed road, constituting the main drainage path, passes diagonally from the top right to the down left corner.

The model was constructed by uniform square basic blocks of size 400 m x 400 m merged together, making the model quasi-uniform on larger scales, as shown in Figure 9. The basic block was constructed in order to represent a generic Swedish urban catchment as a whole. Different parts of the block were constructed to represent city centers, apartment areas, commerce-/ and industrial areas and detached house areas respectively, with green belts in between, and roads along two sides. Two low points were also inserted into the basic block. The basic block was constructed almost symmetrically mirrored along the diagonal. The side roads were only built on one of the mirrored sides though, completing the square road grid along the block borders first when the blocks were merged together. The basic blocks were also rotated when put together in order to make the city center areas located in two of the corners of the basic blocks to converge into clusters of 4, in order to imitate the general structure of extended urban areas, with accumulation of

closed building structures in suburban nodes. A 20 m wide hardened path was added diagonally through the entire catchment model along the main drainage path, in order to allow a generous water flow. The overall proportion of hardened surfaces (including buildings) was yielded as 38 %, which can be considered representative for a Swedish city (Svenskt vatten, 2011).

6.4 Hydraulic modeling in MIKE 21

The simulations were performed in MIKE 21 Flow Model which is a two dimensional modelling tool for hydrodynamic modelling of overland flow developed by DHI (DHI, 2017). The Hydrodynamic only module was used. The model had a spatial resolution of 10 m, the spatial input was hence constituted by 10 m x 10 m grid cells. The run time was set to three hours, with the rain starting right after the beginning of the simulations. Hence, the simulations continued for one hour after the rain had stopped, in order to catch any delayed flow peaks.

6.4.1 Urban catchment model input

The topographic conditions of the urban catchment model were inserted into the program as a bathymetry grid file. The bathymetry file was constructed from the original topography of the model, but now buildings were included as areas elevated three meters and low points were included as areas submerged one meter. All grid cells along the outer rim of the model area in the bathymetry file were set as true land values, creating a closed boundary where water could not flow in or out from the model area.

Bed resistance as well as infiltration and leakage were defined in the model in two separate grid files, both with only two spatial identities: Hardened surfaces and non-hardened surfaces. Hardened surfaces included roads/streets and other paved areas together with the buildings, while the rest, including low points, were defined as non-hardened surfaces.

The outlet in the down left corner of the catchment model was created as nine grid cells defined as sinks with the capacity of removing water at a rate of 100 m^3/s, which was more than enough for consuming all water flowing along the main drainage path. The nine sinks were placed in an angle around the model corner, just inside the true land values at the boundary.

6.4.2 Rain input

The reference rains were inserted as time series with CDS-rains with a 100 years return period, 2 hours duration and 5 minutes resolution, with rain intensities scaled with different factors for different reference rains.

The test rains were inserted as spatial files, constituted of time series together with files of spatial data. The spatial data consisted of a map with 10 m resolution for every tested scenario, where identities representing scaling factors for rain volumes were mapped on the model area. The scaling factors were rounded to whole percents of the maximum rain volume - 65,2 mm. The identity 1 was given to grid cells in the middle of the Gaussian raincell where the the rain volume was rounded to maximum, the identity 2 was given to surrounding grid cells with a rain volume of 99 % of the maximum in

the middle, identity 3 was given to grid cells with 98 % of maximum rain volume, and so on. The corresponding time series was then constructed with several columns, each corresponding to a certain spatial identity. In the first column, corresponding to identity 1, the original CDS-rain time series, with 100 years return time and 2 hours duration, was inserted. In the second column, corresponding to identity 2, the same CDS-rain was inserted, but now scaled by a factor of 0.99. In the third column, the CDS time series was scaled by a factor of 0.98, and so on. As with the reference rains, the CDS-rain time series had a temporal resolution of 5 minutes.

6.4.3 Other input parameters

The other input parameters in the simulations are listed in Table 8. All parameters except the leakage rate for non hardened surfaces are taken from Olsson (2019).

Table 8: General simulation input parameters.

Parameter	**Set value**
Time step	0.2 s
Drying depth	3 mm
Flooding depth	8 mm
Bed resistance at hardened surfaces	50 $m^{1/3}/s$ (Manning's value)
Bed resistance at non hardened surfaces	2 $m^{1/3}/s$ (Manning's value)
Infiltration type	Constant infiltration with capacity
Infiltration zone extent given as	Percentage of the capacity
Initial water volume in infiltration zone given as	Percentage of the capacity

The infiltration parameters applied for hardened and non hardened surfaces are shown in Table 9:

Table 9: Infiltration input parameters.

Parameter	**Hardened surfaces**	**Non hardened surfaces**
Infiltration rate [mm/h]	0.001	36.000
Leakage rate [mm/h]	0,01	0.40
Porosity	0.01	0.40
Initial water content [% of capacity]	20	20
Depth [m]	0.01	0.30

Constant infiltration with capacity means that the upper layer of the ground is handled as a storage layer, with a certain porosity, depth and initial water content, which water might flow into from the ground and out from by percolating down to the groundwater. The maximum inflow to the layer is described by the infiltration rate, while the maximum outflow is described by the leakage rate. The leakage is simply removing water from the model. If the amount of water on the ground is exceeding the infiltration rate, it will start flooding the area, and if the amount of water flowing into the storage layer is exceeding the leakage rate, it will start filling the storage layer. When the layer is filled, water cannot infiltrate any longer.

The leakage rate in reality varies depending on soil type, and is much higher for granular soils than for till and clay. Olsson (2019) uses a leakage rate of 180 mm/h for granular soil, 0.4 mm/h for silt and clay, and 0.36 mm/h for till. In most of Sweden, till

(moraine) is the most common soil type. Clay is also common in the denser populated areas in South and Middle Sweden. In the largest cities, Stockholm and Gothenburg, clay and exposed bedrock (*swedish: berg i dagen*) or very sparse ground cover dominates, in northern Stockholm also till. In areas with sparse ground cover or exposed bedrock, leakage rates can be expected to be very low. Granular soils, constituted by fluvio-glacial sediments, are found in many places in Sweden, including the largest cities, but they make up a relatively small portion of the overall area. As they however have much higher leakage capacity than all other soils, it is hard to conclude by how much they raise the mean leakage rates. As a compromise, 0.4 mm/h was chosen as leakage rate representable for non hardened surfaces in larger Swedish cities. For discussion on other infiltration parameters, time step, flooding and drying, and bed resistance parameters, we refer to Olsson (2019).

6.5 Tested scenarios

All test rains were simulated with the major axis of the gaussian rain intensity distribution oriented along the main drainage path diagonally from the top right to the bottom left corner of the model. For a visual representation of the positioning of the test rains on the urban catchment model in the simulated scenarios, see Figure 10.

6.5.1 Area centric scenarios

Each of the three test rains (test rain 1, 2 and 3) were simulated once with the spatial intensity maximum centered in the middle of each catchment (A, B, C and D). Hence, 12 area centric scenarios were simulated in MIKE 21, one for each test rain and catchment size. All these scenarios were compared with simulations with spatially uniform reference rains, both mean reference rain and maximum reference rain.

6.5.2 Outlet centered scenarios

In addition to this, all three test rains were simulated centered around the outlet of catchment A, B and C for comparison with the maximum and mean reference rains. The rains centered in outlet A coincided with the simulation of test rains centered in mid area B and the rains centered in outlet B coincided with simulation of test rains centered in mid area D, see Figure 10. Simulations were additionally made for each test rain centered in outlet C.

Catchment D was excluded from the outlet centered scenarios since the area surrounding that outlet differs from the areas surrounding the other catchment outlets. There are several sink cells which take water out of the model as well as impermeable border cells, close to the transect used for calculating the outflow. This is not the case for any of the other catchment outlets, which are located well in the interior of the model area.

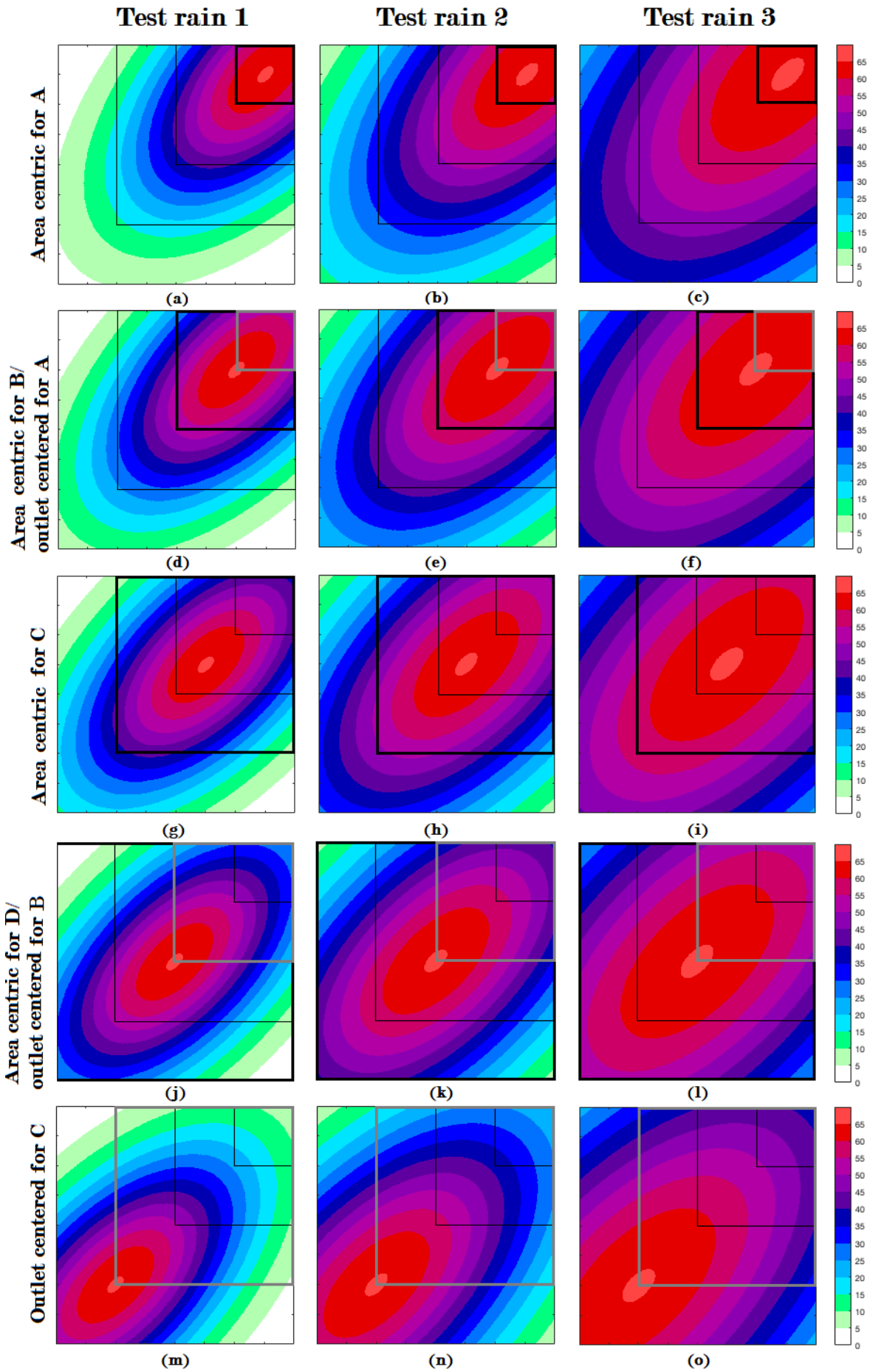

Figure 9: The distribution of rain volume in mm over the urban catchment model, for

the investigated test rain scenarios. The catchment areas investigated for the area centric scenarios are highlighted with a bold black border, while the catchment areas investigated for the outlet centered scenarios are highlighted with a grey border. Other catchment borders are shown with thin black lines. (a) Test rain 1 in the area centric scenario for catchment A. (b) Test rain 2 in the area centric scenario for catchment A. (c): Test rain 3 in the area centric scenario for catchment A. (d) Test rain 1 in the area centric scenario for catchment B and the outlet centered scenario for catchment A. (e) Test rain 2 in the area centric scenario for catchment B and the outlet centered scenario for catchment A. (f): Test rain 3 in the area centric scenario for catchment B and the outlet centered scenario for catchment A. (g) Test rain 1 in the area centric scenario for catchment C. (h) Test rain 2 in the area centric scenario for catchment C. (i): Test rain 3 in the area centric scenario for catchment C. (j) Test rain 1 in the area centric scenario for catchment B and the outlet centered scenario for catchment A. (k) Test rain 2 in the area centric scenario for catchment D and the outlet centered scenario for catchment B. (l): Test rain 3 in the area centric scenario for catchment D and the outlet centered scenario for catchment B. (m) Test rain 1 in the outlet centered scenario for catchment C. (n) Test rain 2 in the outlet centered scenario for catchment C. (o) Test rain 3 in the outlet centered scenario for catchment C.

6.6 Evaluation parameters

6.6.1 Basic hydraulic response parameters

Average maximum water depth
The spatial average of the maximum water depth during the simulation, over a certain area. This parameter was obtained from the statistics output file of each simulation, in a layer where each pixel showed its maximum water level during the simulation.

Proportion flooded area
Here, flooding is defined as water depth reaching 0.1 m or more. This parameter shows the proportion area with maximum water depth of 0.1 m or more during the simulation, for a certain area. It was calculated from the same output file as the average flooding depth, by counting the number of grid cells with maximum water depth of 0.1 m or more.

6.6.2 Evaluation parameters for comparing with both maximum and mean reference rain

Outlet centered scenarios
For comparing the test rains centered in each catchment center with the maximum reference rain, the *Average maximum water depth* and *Proportion flooded area* were obtained for a square area of 500 m x 500 m, closest upstream respective outlet, constituting the part of the catchment closest to its outlet. So, for the test rains centered in the outlet of catchment A for example, the above parameters were obtained for the 500 m x 500 m square furthest downstream catchment A, closest to its outlet.

For the outlet centered test rains, the *Peak outflow* through the outlets of respective catchment were also obtained. The Peak outflow was calculated with the MIKE 21 Discharge calculation tool, by calculating the discharge through a transect of 8 grid cells diagonally over the main drainage path at each outlet. The tool obtained a time series of the water flow through the transect with 5 minutes resolution. The value from the time step with the highest discharge was chosen as the peak outflow. So, for the test rain centered in the outlet of catchment B, for example, the peak outflow was obtained from a transect diagonally over the main drainage path, close to the outlet of catchment B, at

the down left corner of the catchment. The peak hydraulic responses of each catchment outlet were also obtained from the maximum reference rain, for comparison

6.6.3 Evaluation parameters for comparing with maximum reference rain

Area centric scenarios

For comparing the test rains centered in each catchment center with the maximum reference rain, the average maximum water depth and proportion flooded area were obtained for each corresponding entire catchment area. So, for the test rains centered in catchment A, the basic parameters described in 6.6.2 were calculated over the entire catchment A, for test rains centered in catchment B, the parameters were calculated for entire catchment B, and so on. These responses were then compared with the corresponding responses of the maximum reference rain, for the same catchment areas.

6.6.4 Evaluation parameters for comparing with mean reference rain

For the Gaussian test rain comparisons with mean reference rain the following evaluation parameters were used.

Spread ratio

To see how flooding differs inside the catchment area a parameter called spatial ratio is used. The spatial ratio is defined for either the mean flooding depth or proportion flooded area in the central 500 m x 500 m area divided by the mean flooding depth or proportion flooded area in the peripheral 500 m x 500 m area located in the top left corner of each catchment and can be seen in Equation 5. Figure 11 shows where the peripheral and central areas are situated in catchment D. The spatial ratio is calculated from equation 5.

$$SR = EC/EP \tag{5}$$

where SR is the spatial ratio, EC is the evaluation parameter in the central area and EP is the evaluation parameter in the peripheral area.

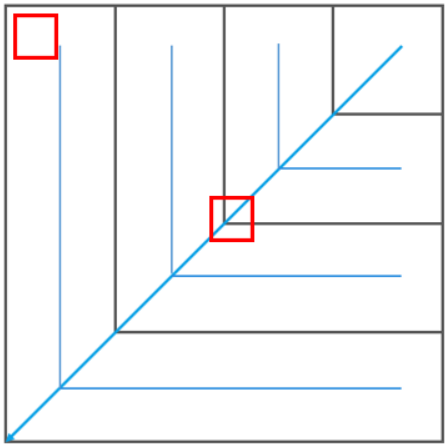

Figure 10: Example for catchment D (the entire urban catchment model), showing the position on the catchment model of the peripheral (upper left corner) and central (middle) evaluation areas as red squares.

To compare the flooding difference within a catchment between the test rains and their corresponding mean reference rain, the spatial ratio of the test rain is divided by the spatial ratio of its corresponding mean reference rain. This ratio is called Spread ratio and calculated according to Equation 6

$$SPR = SR_{TR}/SR_{MR} \tag{6}$$

where SPR is the Spread ratio, SR_{TR} is the spatial ratio for test rain and SR_{MR} is the spatial ratio for mean reference rain.

Catchment/rain-size factor
A driver of the difference in hydraulic response between Gaussian test rains and their mean reference rains is the difference in size between the test rain and the catchment it is raining on. Bigger size differences is expected to give greater differences for the hydraulic responses between the rains. Therefore a factor which shows the size relationship between the test rains and the catchment they rain on was constructed. The factor called Catchment/rain-size factor is calculated in accordance to Equation 7.

$$CRF = Lc/Lr \tag{7}$$

where CRF is the Catchment/rain-size factor, Lc is the length of the side of a catchment, Lr is the relative length of the shortest side of a Gaussian test rain.

7 Results

7.1 Gaussian test rains compared with maximum reference rain

Here the results of the comparison of Gaussian test rains with the reference rain holding maximum rain volume (62,5 mm during 2 hours, corresponding to a rain with 100 years return period) uniformly over the whole catchment areas, are presented.

7.1.1 Area centric Gaussian test rains

Here, results are presented for the Gaussian test rains centered at the middle of each catchment, compared with the spatially uniform maximum reference rain.

The maximum reference rain gave similar responses no matter the size of the catchment, with average maximum water depth slightly below 5 cm and proportion flooded area slightly above 9 %, shown in Table 10. A slight increase in proportion flooded area with larger catchment area can be observed, though.

Table 10: Hydraulic responses to maximum reference rain, for comparison with area centric Gaussian test rains.

Catchment area	**Average maximum water depth** [m]	**Proportion flooded area** [%]
A (4 km^2)	0.0479	9.11
B (16 km^2)	0.0481	9.21
C (36 km^2)	0.0482	9.34
D (64 km^2)	0.0482	9.37

In order to compare the results of the test rains, their responses has been normalized by dividing with the respective response to the maximum reference rain. In Figures 12-14 below, the normalized hydraulic responses to the three test rains are shown as function of catchment size.

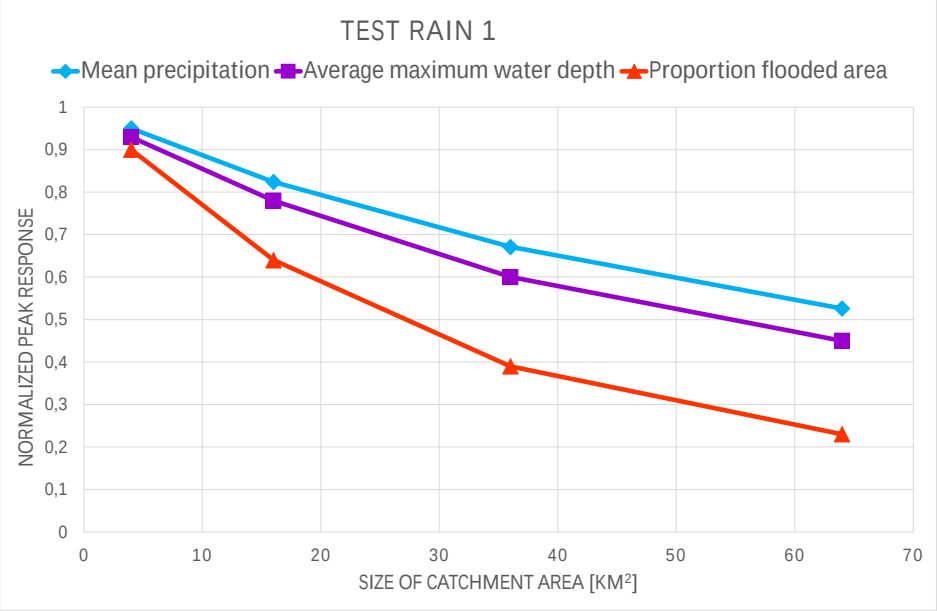

Figure 11: Normalized hydraulic responses and average rain volume for test rain 1 as function of catchment area

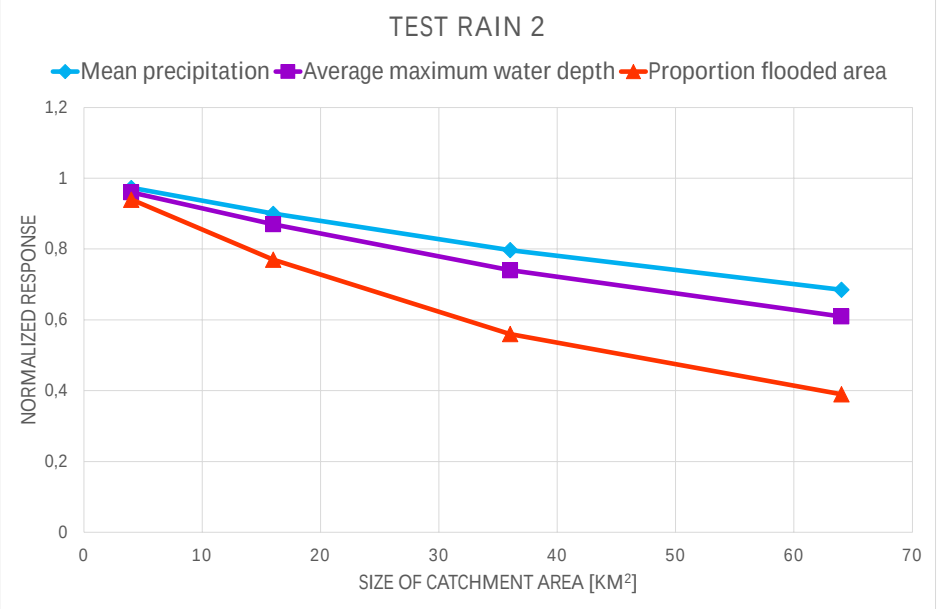

Figure 12: Normalized hydraulic responses and average rain volume for test rain 2 as function of catchment area.

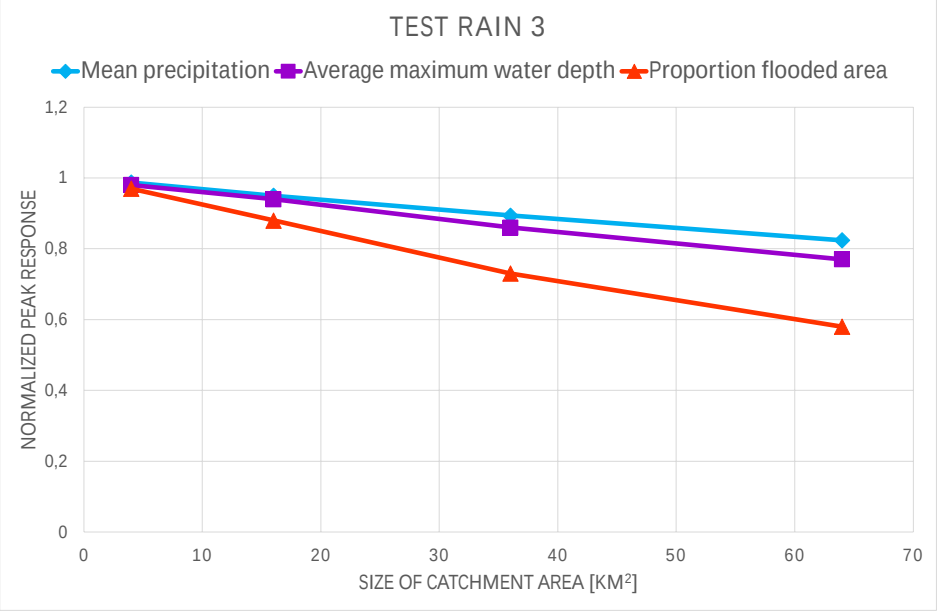

Figure 13: Normalized hydraulic responses and average rain volume for test rain 3 as function of catchment area.

The results show clearly how the normalized responses decrease with catchment size. The effect is the opposite for the relative size of the test rains. The smaller the spatial rain extent, the smaller the hydraulic response. Test rain 1 has the smallest spatial extent and the highest spatial variation, while test rain 3 has the largest spatial extent and the lowest spatial variation. As seen in Figures 12-14, the decrease in normalized peak responses with area is largest for test rain 1, smaller for test rain 2, and smallest for test rain 3. As shown in the same figures, the tested hydraulic parameters seem to decrease faster than the rain volume. The mean water depth only decreases slightly faster than the rain volume, while the proportion flooded area decreases much faster. A possible reason for this could be threshold effects in the hydraulic system. As seen in the figures, all the parameters seem to be smooth functions of catchment size.

All tested parameters are overestimated in the maximum reference rain, when compared with spatially varied test rains. The effect is amplified with smaller raincells (more spatial variation) and larger catchment area. This is strongly expected, since the average rain volume decreases with smaller raincells and larger catchment areas.

7.1.2 Outlet centered Gaussian test rains

Here, results are presented for the Gaussian test rains centered at the outlet of each catchment, compared with the spatially uniform maximum reference rain. The peak outflow through the outlet, together with the average maximum water depth and the proportion area flooded with at least 1 dm water during some time of the simulation, in a square area of 500 m x 500 m closest to the outlet, are considered. The results for the maximum reference rain are shown in Table 11. As seen in the table, all hydraulic

responses to the maximum reference rain are basically independent of the size of the catchment area, with peak outflows close to 3.25 m^3/s, average maximum water depths close to 7 cm and proportions flooded area close to 26 %.

Table 11: Hydraulic responses for maximum reference rain, for comparison with outlet centered Gaussian test rains. Average maximum water depth and proportion flooded area applies for a square area of 500 m x 500 m closest upstream the outlet of respective catchment area.

Catchment area	**Peak outflow** $[m^3/s]$	**Average maximum water depth** [m]	**Proportion flooded area** [%]
A (4 km^2)	3.25	0.070	26.1
B (16 km^2)	3.27	0.070	26.1
C (36 km^2)	3.25	0.069	26.0

As for the outlet centered scenarios, the hydraulic responses to the test rains centered around the outlets were normalized by dividing by the corresponding hydraulic response to the maximum reference rain. The results for each test rain are shown in Figures 15-17, as functions of the catchment area.

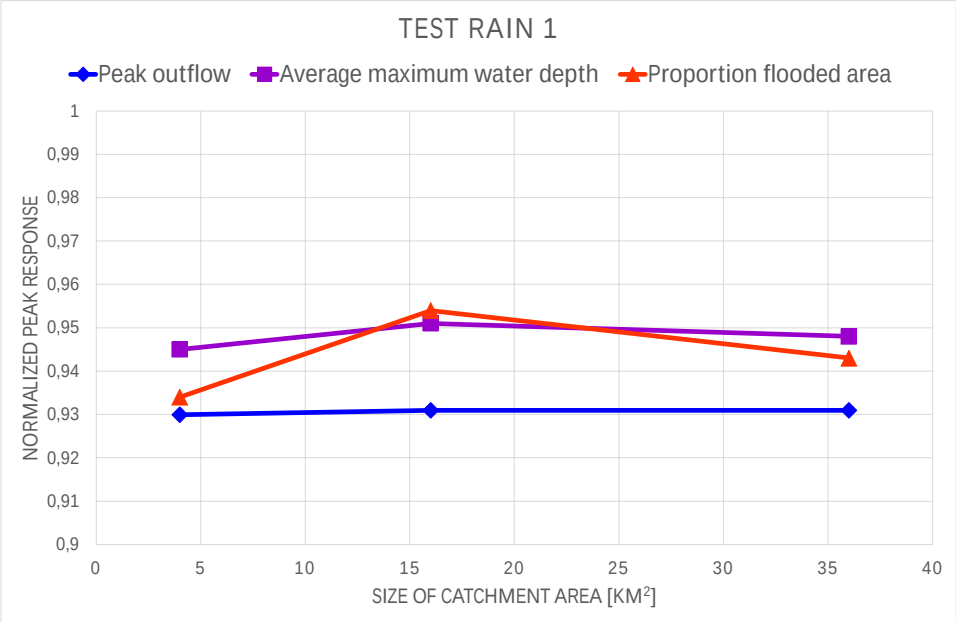

Figure 14: Normalized hydraulic responses and average rain volume for test rain 1 as function of catchment area.

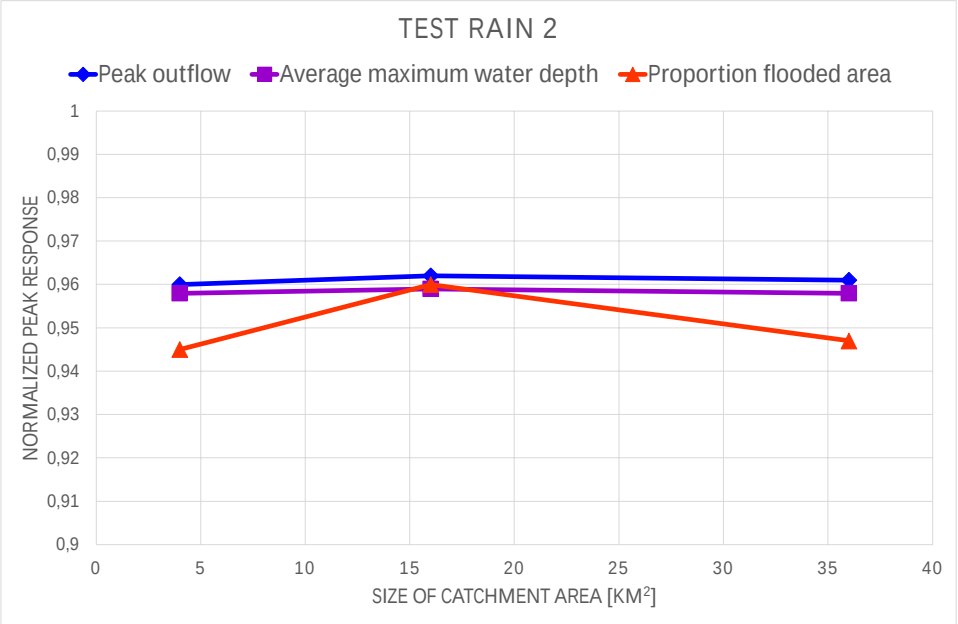

Figure 15: Normalized hydraulic responses and average rain volume for test rain 2 as function of catchment area.

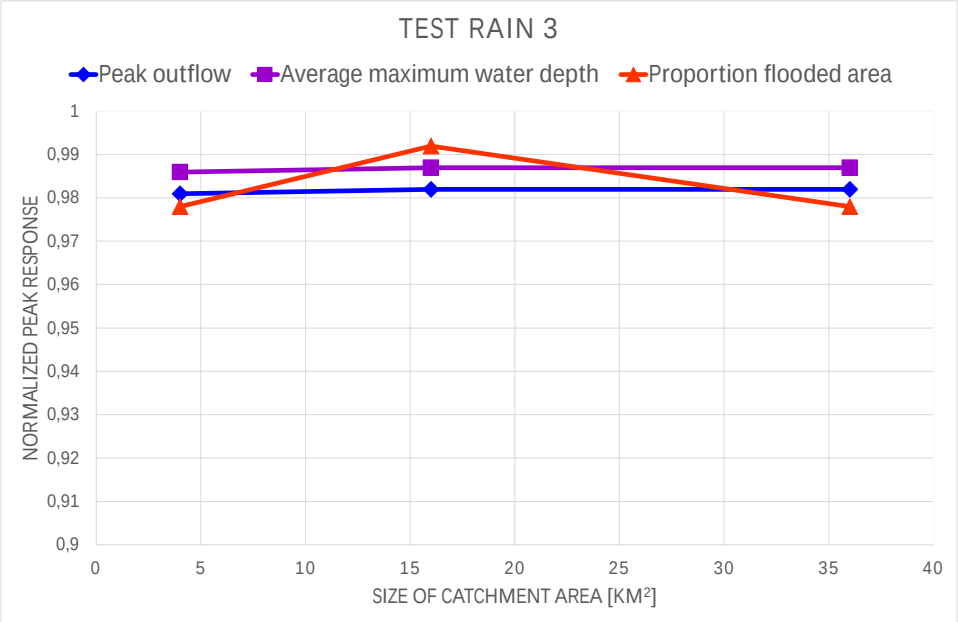

Figure 16: Normalized hydraulic responses and average rain volume for test rain 3 as function of catchment area.

It is hard to recognize any clear trend in the normalized responses with regard to catchment size for any of the test rains, as the lines in Figures 15-17 are more or less horizontal. Catchment B shows a slightly higher proportion flooded area for all rains, but this is most likely a model technical deviation. Test rain 1 shows the lowest normalized responses, around 0.93 - 0.95, as seen in Figure 15. The differences between the test rains and the maximum reference rain slightly decreases with larger and less spatially varied test rains. Accordingly, test rain 2 shows slightly higher normalized responses, around 0.95 - 0.96, as seen in Figure 16. Test rain 3 shows the highest normalized responses - as seen in Figure 17 around 0.98 - 0.99, so very close to 1. Hence, the hydraulic response to test rain 3 differs very little from that to the uniform reference rain, regardless of the catchment size.

The results show clearly that the spatial variation of the rain has limited effect on the hydraulic response, no matter the size of the catchment. For all tested hydraulic parameters, test rain 3 differed around 1-2 % from the uniform reference rain, test rain 2 around 4-5 %, and test rain 1 around 5-7 %. The values hardly change with catchment size.

The normalized peak outflow plotted against catchment size for all three test rains is shown in Figure 18 below. It clearly shows how the normalized responses seem more dependent on the spatial variation of the test rain than on the catchment size. Test rain 3 shows responses very similar to the reference rain, with normalized peak outflows constantly around 0.98. Test rain 2 shows slightly lower normalized values, close to 0.96, while test rain 1 gives normalized peak outflows close to 0.93.

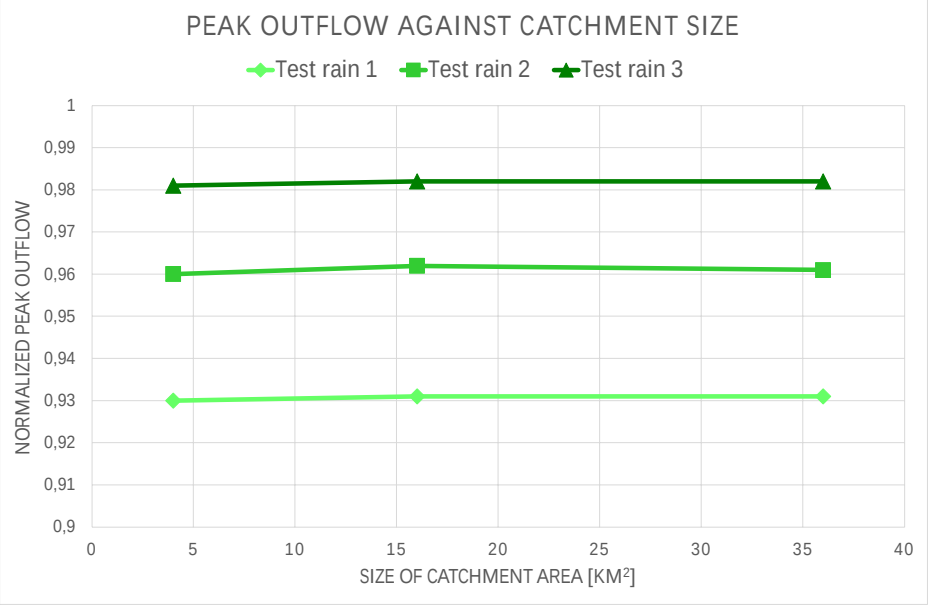

Figure 17: Normalized peak outflow for the three test rains centered around respective outlets, as function of catchment area.

In Figure 19, the normalized peak outflow from each catchment is plotted against the relative cell size of the test rains, with width 4, 5.5 and 8 km, respectively.

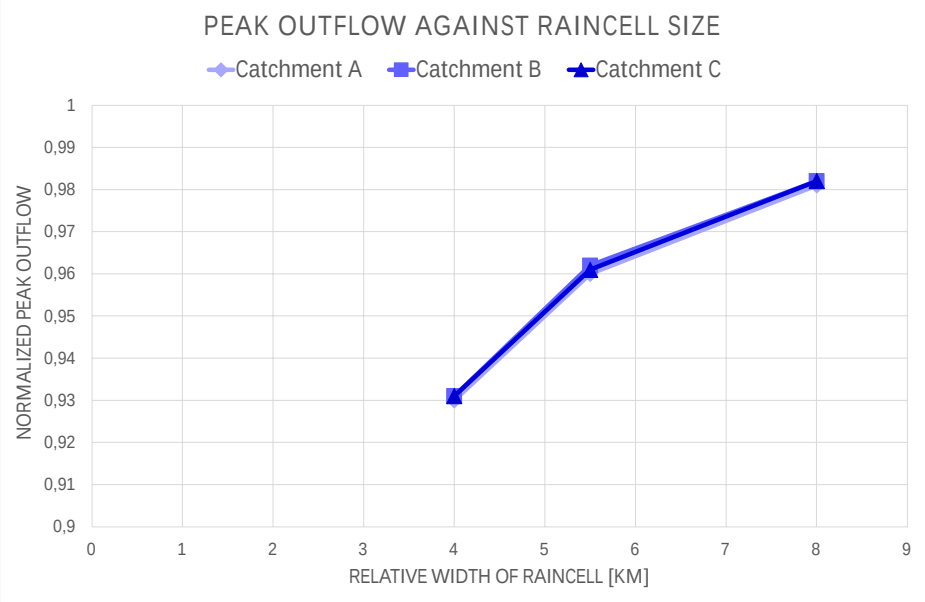

Figure 18: The normalized outflow from each catchment as function of the relative cell width of the test rains.

The plot clearly shows how the normalized peak flows depend on the size of the raincells rather than on the catchment size. The differences between the different catchment sizes are hardly visible at all, as the lines representing the different catchments follow almost exactly the same path. For the peak flows to differ with more than 5 % from the maximum reference rain, the relative cell width of the raincells needs to become lower than around 5 km. With increasing cell sizes, the normalized response is approaching 1.

7.2 Gaussian test rains compared with mean reference rains

Here the results of the comparison of Gaussian test rains with the reference rains holding mean rain volume uniformly over the whole catchment areas, are presented.

The ARF values corresponding to the scaling factor between maximum reference rains and mean reference rains are presented in Table 12. These values are calculated from the average rain volume of a test rain centered in the middle of a catchment divided by the maximum rain volume of the test rain.

Table 12: The ARF values of every rain and catchment combination given by the average rain volumes of the test rains divided by the maximum rain volume of the test rain.

Test rain and catchment	**ARF values**
test1-A	0.95
test1-B	0.83
test1-C	0.67
test1-D	0.53
test2-A	0.97
test2-B	0.90
test2-C	0.78
test2-D	0.68
test3-A	0.99
test3-B	0.95
test3-C	0.89
test3-D	0.82

The ARF values in Table 12 show that smaller test rains placed on larger catchments give lower ARF values. This is expected since the rain volume of Gaussian test rains decreases with distance from the raincell centre and the rate of the rainfall decrease is caused by the spatial variation of the rain. With larger catchments relative to the raincell size, a larger proportion of the catchment will be situated in the periphery of the rain, leading to lower mean rainfall over the catchment.

7.2.1 Area centric Gaussian test rains

The results of the hydrodynamic simulations with mean reference rain compared with test rains centered in the middle of each catchment are presented here.

To see how the spread ratio differed between the three test rains and how they depended on catchment size, the spread ratio based on the average maximum water depth as a function of catchment size for all test rains are shown in Figure 20. The spread ratio for proportion of flooded area are shown in a corresponding way in Figure 21.

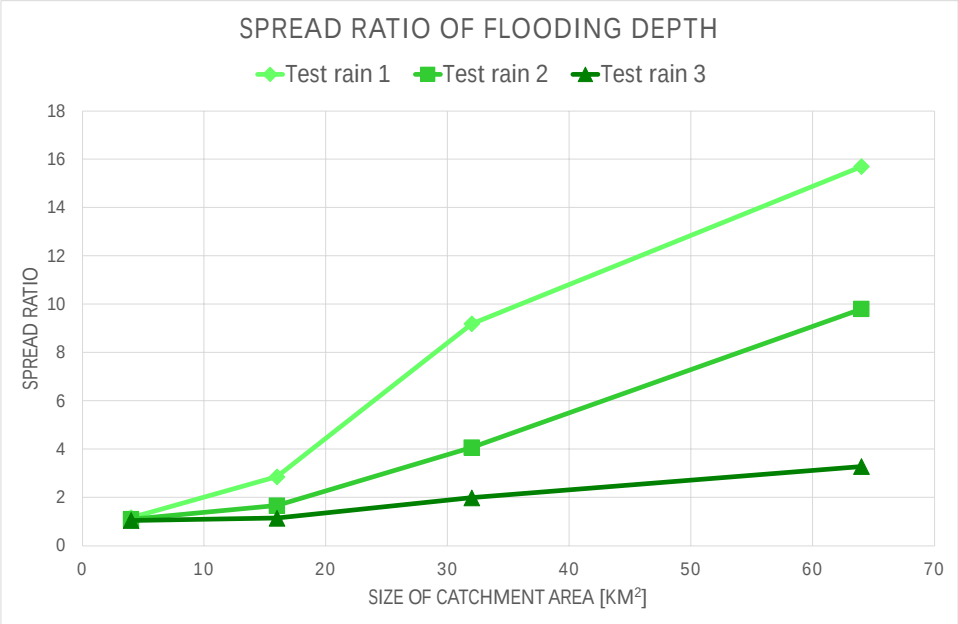

Figure 19: Spread ratio of flooding depths for the three test rains as function of the catchment area.

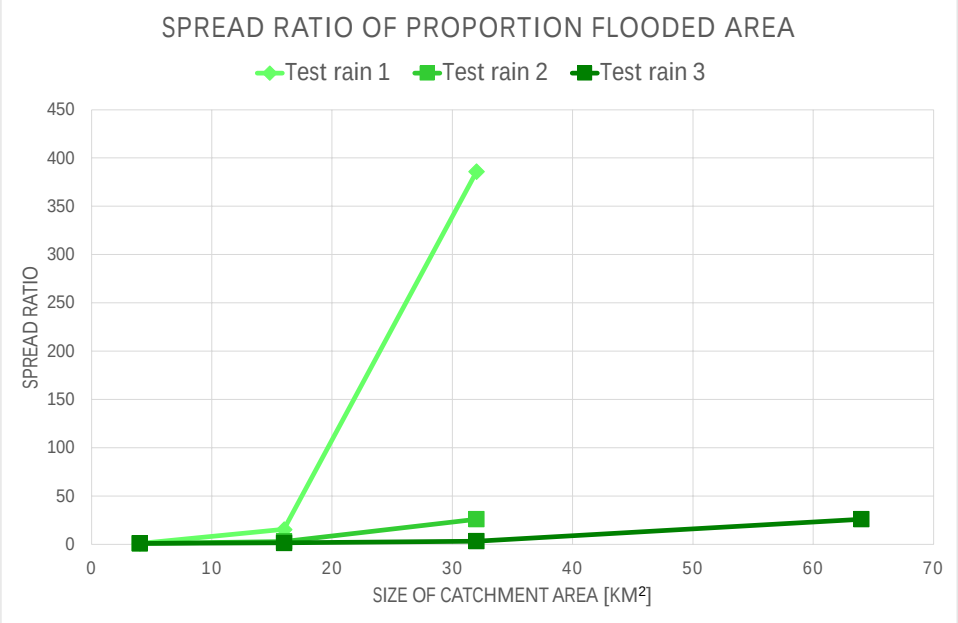

Figure 20: Spread ratio of proportion flooded area for the three test rains as function of the catchment area.

The spread ratio of every catchment and rain combination can be seen in Table 25 in

appendix B. Figure 19 and 20 shows that there was a stronger difference between the central and peripheral areas for the test rains than for the reference rains since the spread ratio is always larger than 1. This difference increased with larger catchments and smaller test rains which is seen by the increase of the spread ratio for larger catchments corresponding to higher values in the x-axis and a steeper slope for the smaller test rains. This is expected since that combination leads to greater spatial rain variability within the catchment. Both evaluation parameters increased with a higher gradient for smaller rains. Proportion flooded area reacted stronger to area increase than average maximum water depth and it reaches infinity for test rain 1 and 2 for catchment sizes greater than B. Only test rain 3 has a spread ratio less than 1.1 in catchment A for both flooding depth and proportion flooded area.

7.2.2 Outlet centered Gaussian test rains

The biggest difference between the hydraulic response to the mean reference rains and the Gaussian test rain should occur when the test rains are centered near the outlet, since the whole catchment is upstream that point. Therefore comparisons of the normalized hydraulic peak responses of reference rains compared with test rains centered in the outlet were performed. The normalized responses were peak outflow at the outlet of each catchment, average maximum water depth in a 500 m x 500 m square closest upstream the outlet and proportion flooded area in the same square.

In order to investigate how the size of both catchment area and Gaussian rain cells influence the hydraulic response difference between a Gaussian test rain and a mean reference rain, Figures 21, 22 and 23 were plotted, where the normalized hydraulic responses of test rain 1, 2 and 3 are plotted against the areas of the catchment they were simulated on.

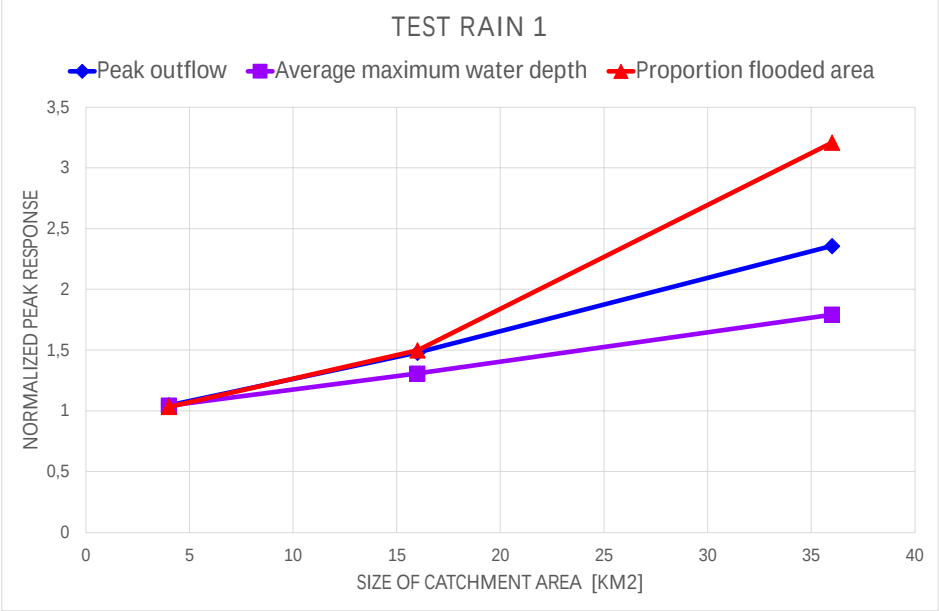

Figure 21: Normalized hydraulic peak responses for test rain 1 centered around the catchment outlet of respective catchment, plotted against catchment size.

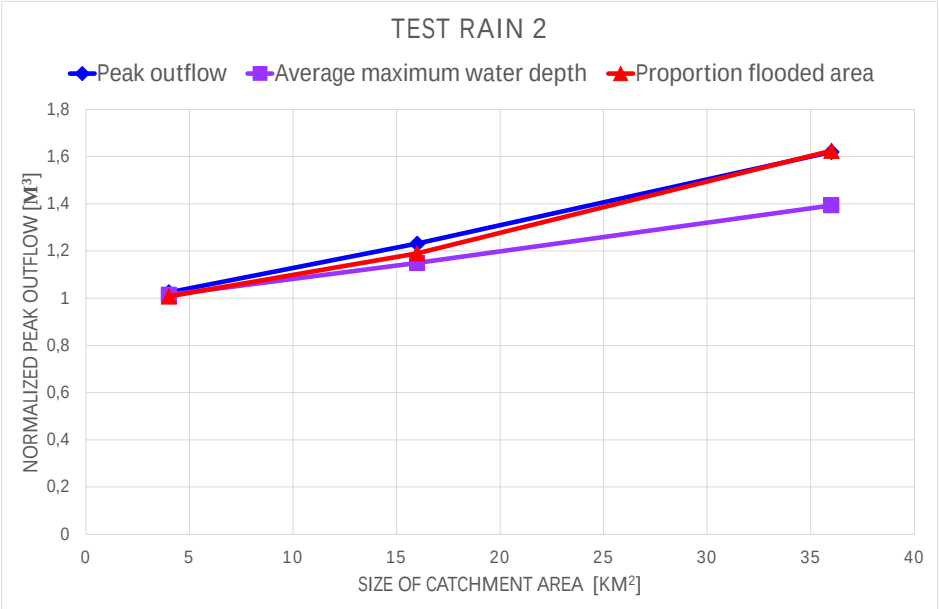

Figure 22: Normalized hydraulic peak responses for test rain 2 centered around the catchment outlet of respective catchment, as function of the catchment area.

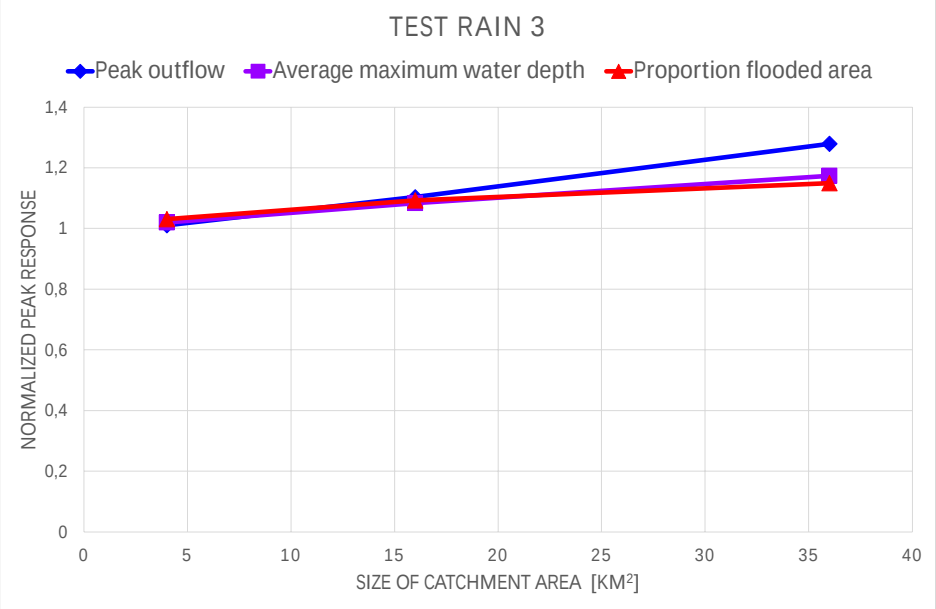

Figure 23: Normalized hydraulic peak responses for test rain 3 centered around the catchment outlet of respective catchment, as function of the catchment area.

Values of the normalized peak responses in the outlet centered scenarios can be seen in Tables 26, 27 and 28 in appendix B. By inspecting the x-axis of figures 22, 23 and 24 it is seen that larger catchment areas give higher normalized peak outflow, and by comparing the normalized peak responses between the different rains, steeper slopes for smaller test rains are seen. The proportion flooded area also seems to be the most sensitive parameter for test rain 1 and 2 which could be caused by threshold effects when many areas reach flooding capacity over a certain point.

In Figure 24 the normalized peak outflow was plotted against the relative width of the test rains to see the influence of catchment- and rain size even clearer.

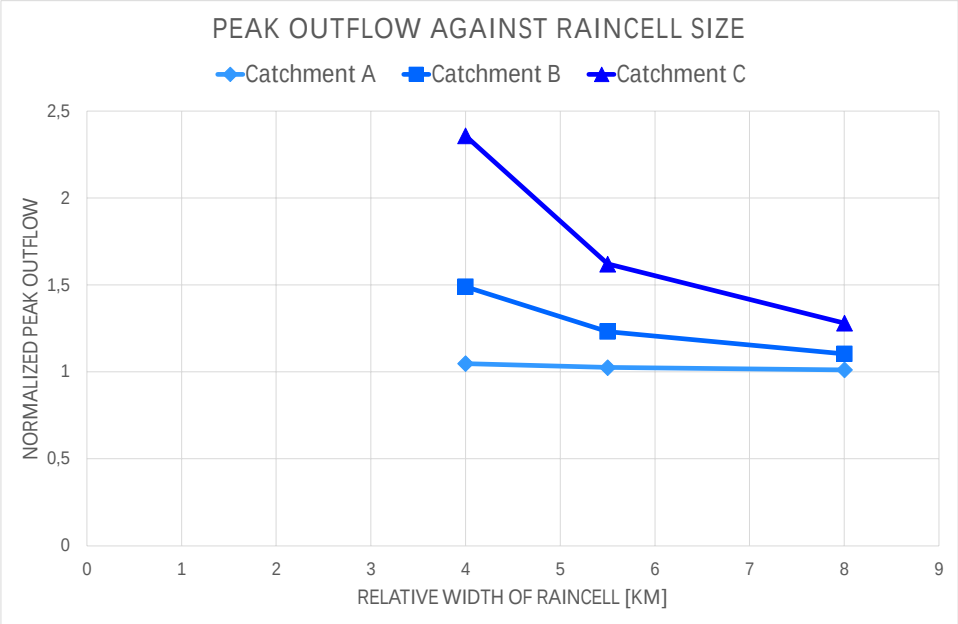

Figure 24: Normalized peak outflow for catchments A,B and C for the test rain centered around the catchment outlet, as function of the catchment area

Figure 24 shows that catchment A only gives a small difference in peak outflow between the test rain and mean reference rain.

The hydraulic peak response to reference rains on catchment A which has an area of 4 km^2 is underestimated with 1-5 % for all of the evaluation parameters compared to the test rains. In catchment area C with the area 36 km^2, the peak responses were underestimated with 13-69 % depending on the evaluation parameters.

The hydraulic evaluation parameters peak outflow, mean maximum water depth, and proportion flooded area were plotted against their Catchment/Rain-size factors seen in Figures 26, 27, and 28 to see how this size relationship affect difference in hydraulic peak outflow between test rains and mean reference rains.

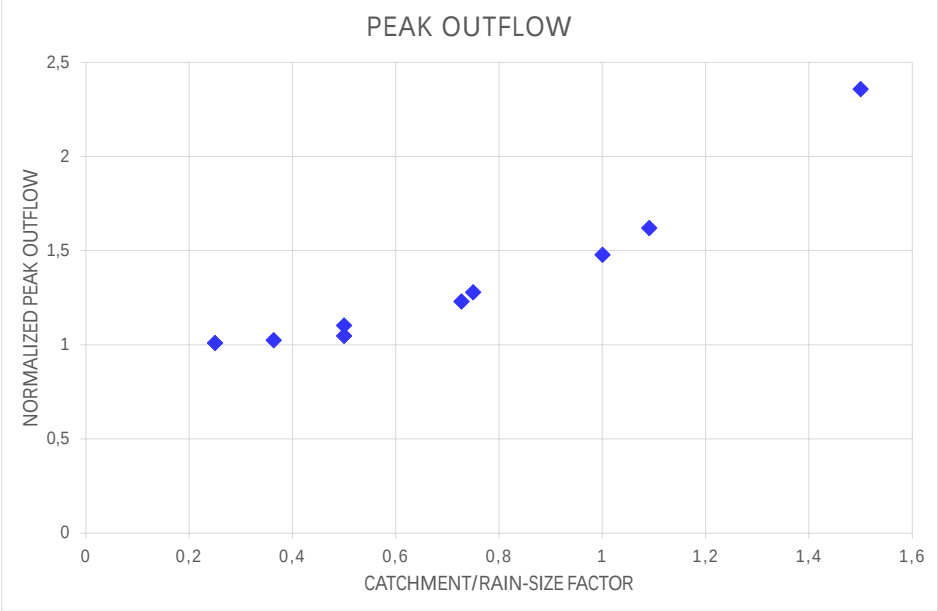

Figure 25: Normalized mean reference values of peak outflow plotted against the Catchment/rain-size factor of every raincell-catchment combination.

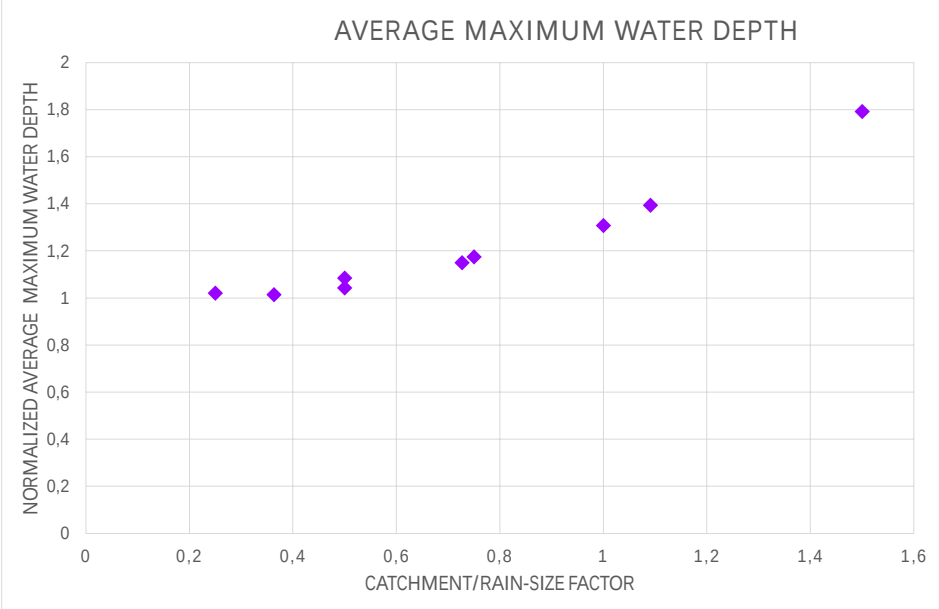

Figure 26: Normalized mean reference values of mean maximum water depth plotted against the Catchment/rain-size factor of every raincell-catchment combination.

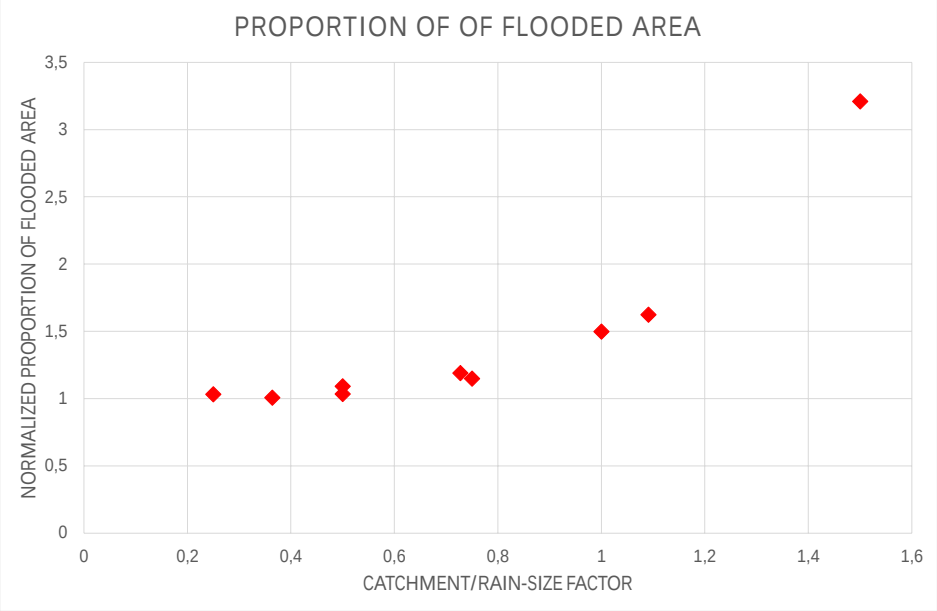

Figure 27: Normalized outflow plotted against the Catchment/rain-size factor of every raincell-catchment combination.

Figures 25, 26 and 27 show a clear relationship between the hydraulic evaluation parameters and the Catchment/rain-size factor. A higher Catchment/rain-size factor gives higher normalized peak responses for every evaluation parameter. All the evaluation parameters with Catchment/rain-size factors of 0.5 or less have a normalized response value of 1.1 or less.

8 Discussion

8.1 Relevant concepts

In order to enable a smooth discussion, we need to introduce two new concepts: *Effective rain duration* and *peak contribution area*.

With *effective rain duration*, the duration of the part of the rain that contributes to the hydraulic peak response is intended. For a rain with intensity constant in time (a block rain), the effective duration will coincide with the total rain duration, but for other hyetographs, this is not necessarily the case.

The *peak contribution area* is the area whose runoff contributes to the hydraulic peak response. Its size is dependent on the effective rain duration. The longer the effective rain duration, the larger the peak contribution area will be.

8.2 Gaussian test rains compared with maximum reference rain

8.2.1 Area centric Gaussian test rains

The values of hydraulic response calculated for area centric Gaussian raincells are average values for entire areas. In practise, the results can be interpreted as using spatially uniform design rains for hydraulic modelling and cloudburst mapping, the simultaneous extent of the hydraulic response can be vastly overestimated. This is somewhat obvious from the beginning. One can ask what such an overestimated simultaneous extent of hydraulic response really matters. We might want to know how often one street is flooded, as well as how often another street, several kilometers away in the same catchment, is flooded. But does it really matter if these two streets are flooded during the same event, or not? One must remember that the return period of a specific rain event is given for any specific point, not for an area. In a large catchment, several raincells corresponding to a 100-year event in the cell core might pass during 100 years, but only one cell core is expected to hit any given specific point during that time. When simulating a rain with 100 years return period, is it then reasonable to simulate such rain simultaneously over the entire area? The answer depends on how much the hydraulic response in every point is affected by the rain that falls in a different part of the catchment area. If the hydraulic response is propagating effectively through the catchment, a spatially uniform (simultaneous) design rain would overestimate the hydraulic response. In order to answer this question, the simulations of gaussian test rains centered in the outlet of each catchment area, were performed.

8.2.2 Outlet centered Gaussian test rains

For this part of the study, the hydraulic response close to the outlet from the three Gaussian test rains centered around each catchment outlet respectively, were compared with the hydraulic response to the maximum reference rain. Accordingly, in all tested scenarios, a rain with 100 years return period was simulated close to the outlet, both in test and reference simulations. In the spatially varied test simulations, the rain volume decreased with distance from the outlet (see Figure 10), while in the maximum reference simulation, it did not. By comparing these, conclusions can be drawn about how much a spatially uniform design rain would overestimate the hydraulic response in the worst affected area, due to overestimated contributions from peripheral parts of the catchment. The investigated hydraulic responses were peak outflow from the catchment, together with average maximum water depth and proportion flooded area (areas with 0.1 m water depth or more during some time of the simulation) in a square area of 500 m x 500 m closest upstream the outlet of each catchment.

The results show clearly that the spatial variation of the rain has limited effect on the hydraulic response, no matter the size of the catchment. For all tested hydraulic parameters, the test rains differed between 1 and 8 % from the uniform reference rain. The values hardly changed with catchment size.

Regarding the results, it is important to consider what the Gaussian test rains really represent: Test rain 3 represents a relatively large cumulative raincell, with a relative width approximately corresponding to the 60th percentile, from the analysis of precipitation radar data. Test rain 2 represents approximately the most common sized observed

cumulative raincell, corresponding to the 30th percentile regarding relative width, while test rain 1 represents a very small cumulative raincell, with the smallest observed width from the study. Hence, the conclusion can be drawn that, using spatially uniform design rains, the hydraulic response of around 60 percent of the real events can be expected to be overestimated with around 1-2 % or more. Around 30 % can be expected to be overestimated with around 4-5 % or more. Very few events can be expected to be overestimated with more than around 5-8 % or slightly more. This seems to apply no matter the size of the catchment, as long as it is at least 5 km^2. The exact numbers stated above are in reality unsure, but the results still speak clearly, and these results are what really matters for practical implications. The areal parameters, which describe the amount of water on the ground, are of high importance for cloudburst mapping, while the peak flows are of crucial importance for dimensioning of hydraulic infrastructure, like pipes and culverts.

To summarize, the difference in hydraulic peak response between real events and a spatially uniform design rain seems to be small for most rains. For many practical implications, the difference might be considered negligible. Hence, it is estimated to be a limited need for taking spatial variation of rains into consideration when performing cloudburst mapping for peak responses in Swedish urban areas.

The reason for this, somewhat unexpected, result summarized above, is that in large catchments, the hydraulic response does not have time to propagate through the whole area during the simulated rain duration, of 2 hours. When the catchment is larger than the peak contribution area, the rain that falls far up in the catchment does not reach the outlet in time to contribute to the peak response, so that response would hardly change, no matter how large the catchment area and the rain extent is. The spatial variation of the rain only matters for the peak response if the rain has a significant variation within the peak contribution area. Smaller raincells than those tested in this study are required in order to accomplish large differences in rain amount over the peak contribution area, and hence large differences in hydraulic response. According to the radar analysis, no such small cumulative raincells were observed, and they can accordingly be supposed to be very unusual. Only test rain 1 managed to accomplish a decrease in peak responses with more than 5 % in comparison to the uniform reference rain.

The above explanation of the results can be compared with one of the basic assumptions made in the so-called rational method, a statistical method traditionally used for estimating peak outflows from catchments. The method uses the assumption that the maximum outflow is achieved when the rain duration coincides with the time of concentration (Lyngfelt, 1981). The time of concentration is the longest time it takes for water to reach the outlet from any point in the catchment. In the rational method, a rain constant in time is assumed, which results in an effective rain duration equivalent to the total rain duration. Using the concepts described in this report, the rational method states that the maximum outflow is obtained exactly when the peak contribution area reaches the size of the total catchment area.

The conclusion can be drawn that, if a catchment is larger than the peak contribution area, the hydraulic peak responses will no longer be dependent on the catchment size. Since the normalized responses hardly change with catchment size for any of the rains tested in this study, this criteria can be assumed to be met for all tested catchment sizes.

The normalized responses can be expected to be 1 in a catchment small enough, then decrease with catchment size, until the catchment reaches the size of the peak contribution area, and then level off to a constant value. Such normalized responses constant with catchment area is what this study provides. Investigating the properties of this decrease before the constant value is reached, might be a subject for further studies using smaller catchments.

The results of this part of the study can be compared with a danish study recently made by Thorndahl et al. (2019), using radar data from Själland and Southwestern Skåne to determine ARF:s. Considering the geographical closeness and a similar summertime climate, the properties of convective precipitation in the Öresund region can be expected to be little different from those in most of Sweden. The radar data used in that study had a resolution of 500 m x 500 m, compared with 2 km x 2 km in this study. The danish study showed stronger spatial variation of rains than this study concluded, with the mean ARF comparable to test rain 1 - representing extremely small raincells according this study. The higher resolution of the analysed radar data might possibly be a part of the explanation. Thorndahl et al. (2019) concluded that a uniform design rain of 1 h duration, without ARF could be expected to overestimate the rain intensity with around 25 % for a 10 km^2 catchment. This can be compared with around 1-8 % found for rains with 2 h duration, centered around the outlet, in this study. The difference in duration cannot explain the great difference between the two studies, instead an important reason is the stronger spatial variations of rains found in the danish study. The latter also differs from this study in the sense that it does not simulate the hydraulic response on the ground. Instead it uses the same simplified assumption as in the rational method discussed above, and concludes its result on a 10 km^2 catchment based on the assumption that such a catchment has a time of concentration of 1 hour, and hence consider a rain with a duration of 1 hour.

The size of the peak contribution area is dependent on the distance that water can elapse during the effective rain duration. This distance depends on the effective rain duration and the flow speed of the water, which in turn depends on the roughness of the surface, the slope, and also the rain intensity (Lyngfelt, 1981). With more rain, and hence more water on the ground, it can flow faster. For a simplified adoption, the flow speed of the water can be approximated to 0.1 m/s along paved streets. In that case, the water will elapse 720 m during 2 h, the duration of the rain used here. As a comparison, the smallest catchment area in this study (catchment A) is a 2 km x 2 km sized square. In order to travel diagonally through catchment A during the rain duration, the water needs an average speed of almost 0.4 m/s. That is not impossible in an extreme rain, but it is unlikely for the water to travel through catchment B, with double the size of A, during the same time. In accordance, there is hardly any difference in normalized peak response between the different catchment sizes. In comparison, the assumption that a 10 km^2 catchment has a time of concentration of 1 hour made by Thorndahl et al. (2019), presumes a much faster water flow.

A parameter that could change the obtained result is the topography of the model. A steeper topography with steeper drainage paths would give faster running water and a faster runoff process, where larger parts of the catchment could contribute to the peak hydraulic response. In other words, the size of the peak contribution area increases with

steeper topography, and might possibly exceed the sizes of the tested catchments. This would imply larger differences between the spatially varied Gaussian rains and the spatially uniform reference rain, and result in larger overestimations when using a spatially uniform design rain. According to the Manning formula, shown in Equation 8:

$$v = MR^{2/3}\sqrt{I} \tag{8}$$

where I is the slope, R is the hydraulic radius, and M the Manning number, the flow speed (v) will increase with the square root of the slope. The Manning formula is normally used for water flow in pipes and channels. The TR-55 report, often used for design purposes, uses Manning's kinematic solution to calculate travel time for sheet flow of shallow water on the ground, where the travel time is inversely dependent on the slope to a power of 0.4 (USDA, 1986). Since velocity is inversely related to travel time, the velocity will then be dependent on the slope to a power of 0.4. The basic slope dependence hence remains almost unchanged in comparison to the Manning formula, with close to a square root dependence on the slope. With flow velocity proportional to the square root of the slope, a large change in slope is needed to obtain a significant change in flow speed, which decides the size of the peak contribution area, for a given rain duration. To obtain a doubling of the water speed, a quadrupling of the slope is needed. With the small differences in hydraulic peak responses between test and reference simulations obtained here, a much steeper terrain than in this model is probably needed for giving a pronounced difference. In addition, the straight and relatively broad paved main drainage path in the model is facilitating an unimpeded flow along it. In real cities, drainage paths can be expected to have more complicated structures, which might obstruct a fast water flow over longer distances. With this into consideration, even steeper terrain might be needed. Probably, a topography with much larger relative height differences than in the model used in this study is needed to give significant differences in hydraulic responses between most real events and a uniform design rain with maximum intensity everywhere. Most larger Swedish cities do not exhibit a topography with much larger relative height differences than used in the model. For further discussion on the model topography, see section 8.4.2.

8.3 Gaussian test rains compared with mean reference rains

8.3.1 ARF relevance

Areal reduction factors are used to represent estimates of average areal rainfall from statistics of point rainfall, in order to represent real rainfall better. The ARF reduces the rainfall increasingly for larger sizes of the catchments which the rain is applied on, since the average areal rainfall decreases with catchment size.

Common practise in Sweden today is to only use ARFs for rural areas and for rains of long durations. But there might be a case for them to be implemented in urban cloudburst mapping as well. The usefulness of ARF-scaling design rains was therefore investigated in this study.

The method used in this study for estimating ARFs was most alike the storm centered approach, but over catchment areas instead of areas specific to the raincell. The ARF values are based on the mean cumulative rainfall of the Gaussian test rains, over the

catchment it is stationed on, divided with the maximum rainfall at the center of the raincell. By using a strict storm centered approach, dividing the mean rainfall within one or more standard deviations of the rain or other area sizes related to the size of the rain, with the maximum rainfall, would give the ARF value of that storm regardless of the shape of a catchment. With this method, an equation can be made where an ARF value can be chosen by inserting an area value as input. But since this study focused on the designed urban Swedish catchment model, ARF values for the catchments in that model were deemed sufficient.

Sizes of convective rainfall varies between climatic regions and the spatial nature differs greatly between different rains such as frontal and convective rain. Hence, the type of rainfall data and the climatic region which the data is measured from determines where the ARF is applicable. The mean reference rains in this study only uses data of convective rain cells from events with high amount of recorded precipitation, during 2 hours from Sweden. Dahlström (2010) states that extreme short-term precipitation in Sweden almost exclusively come from convective raincells. Hence the ARF values obtained from this study should be more applicable for Swedish cloudburst mapping than ARF values based on data from other climatic regions or based on other types of precipitation.

8.3.2 Validity of ARF values

As stated in section 2.6, a recent study from Denmark by Thorndahl et al. (2019) estimated ARF values with a storm centric approach. They used 15 years of high resolution radar data with 500 m x 500 m resolution from Själland and southwestern Skåne to create estimated ARF values as functions of area and rain duration. Since the rain data is partly inside or closely situated to Sweden and the study also uses a storm centric approach from radar data, those values should give an indication of the realisticness of the ARF values from this study. Using their derived function of ARF:s with area and rain duration as input, a comparison could be made. The biggest difference is that the ARF:s for the smaller catchments were smaller for the Danish study. A reason for this could be the higher resolution of their radar data. A finer spatial resolution gives more insight into the spatial variation of the smaller rains which could not be detected in this study which used 2 km x 2 km data resolution. The test rain which had ARF values most similar to mean ARF from Thorndahl et al. (2019) was test rain 2 which relates to the modal value of the cumulative rain cells. This is expected since it is also based on the mean relative size of the rain intensity cells from the analysis of precipitation radar data. The higher values of the ARF from this study corresponding to smaller catchments is higher than than the ARFs from Thorndahl et al. (2019) but they decrease faster than the values of Thorndahl et al. (2019) until the ARF:s of both studies gets close to aligning at the largest catchment size of 64 km^2.

8.3.3 Area centric Gaussian test rains

Contrary to the maximum reference rain, the mean reference rain has the same total amount of rainfall as the test rains over respective catchment. But the amount of rainfall is not all that matters, where the rain falls inside a catchment greatly influences the hydraulic responses. Therefore a comparison of the hydraulic responses of a mean reference rain and a test rain can give insight in to what the mean reference rain misses. How much a mean reference rain would underestimate the hydraulic responses and how this

is affected by catchment size and the spatial variation of the rain in the worst hit areas are important questions, since using spatially uniform rains are common practice today.

The spread ratio was used to measure how hydraulic responses differ within a catchment, between a spatially uniform reference rain and a Gaussian distributed raincell. The proportion of flooded area seems to be the most sensitive parameter for the spread ratio. For test rains 2 and 3, catchments C and D gave no flooded cells in the peripheral areas leading to a spread ratio of infinity. This can be explained by the form of the Gaussian function, which has most of its volume close to the center and then decreases rapidly to continue as an infinitely long tail. For the larger catchments and smaller test rains, the peripheral area falls outside of the main part of the Gaussian raincell, leading to greatly reduced rainfall intensities which inhibits the water to reach flooding depth on the ground.

Only the biggest rain in combination with the smallest catchment gave hydraulic response differences smaller than 10 % between the test- and reference rains, which indicates that the spread of hydraulic response within Swedish catchment are not well represented by uniform design rains.

The spatial extent of the hydraulic response seems to be sensitive for spatial variation of the rain, even in the smallest catchment. However the relevance of this conclusion is limited, since raincells can take many paths through an urban catchment. At least it can be concluded that the spread of rainfall between a uniform and spatially varied rain on Swedish urban catchment do seem to differ. But what should be more important for stormwater management than the difference in spread of rainfall between different rains, should be how much the spatial variability of rain influences the the peak hydraulic responses.

8.3.4 Outlet centered Gaussian test rains

To integrate the role of the sizes of both the catchments and the raincells on the difference in hydraulic response between test and reference rain into one parameter, the *Area/rain-size ratio* was introduced.

For all the evaluation parameters with catchment/rain-size factors of 0.5, the hydraulic responses of the mean reference rains only differed with 10 % or less from those of the test rain. The *relative length of the minor axis* of the test rain is twice the length of the standard deviation of the Gaussian distribution of the test rain. This means that the peak responses within the area worst hit by a raincell can be estimated well with a mean reference rain, if the square root of the catchment size (corresponding to the length of a square catchment) is less than or equal to the standard deviation of the rain. See Equation 9:

R_{std} = *Relative length of the minor axis of the Gaussian raincell*
$\sqrt{A}$ = *Length of a square catchment*

$$R_{std} \geq \sqrt{A} \tag{9}$$

Note that this was the case for a square catchment with a cumulative Gaussian raincell with length-width ratio of 2. But this could be a good indication for other catchments with forms not too oblong.

8.3.5 Explanation of the results

Why does the reference rain always give lower hydraulic response than the test rain placed in the outlet and why does the difference increase with larger catchment sizes as seen in Figures 22, 23, 24 and 25?

The explanation comes from same phenomena which causes the peak hydraulic response to the maximum reference rains to not vary with larger catchment sizes. The peak contribution area for each catchment decides when increased area does not increase hydraulic peak response. So the hydraulic response for a rain with a certain duration should in theory increase with larger catchment areas until the catchment has reached the size of the peak contribution area. At that point the peak hydraulic responses for neither the spatially varied test rains nor the reference rains will increase.

But a crucial difference between the spatially varied test rain and the mean reference rains is that scaling the size of catchment further from the size of the peak contribution area, decreases the amount of rainfall inside the peak contribution area of the mean reference rains, but not of the test rain. Therefore larger areas lead to bigger differences in hydraulic responses. The fact that the smallest catchment of 2 km x 2 km had similar hydraulic peak responses for the mean reference rain and test rains for all evaluation parameters, indicates that the size of this area is close to that of the peak contribution area for every simulated rain.

8.4 General discussion

8.4.1 Relevance of the study

Several earlier studies have explored how catchment size and spatial rain variation influences the hydraulic responses, with diverse results (Arnaud et al., 2002; Brath et al., 2004; Gabellani et al., 2007; Lobligeois et al., 2014; Patil et al., 2014). No study we have encountered has performed this for Swedish conditions, though. As stated in the section 2.6 the size of convective raincells do vary between different climatic regions. Therefore a study specific for Sweden may give results which should be more accurate for Swedish cloudburst mapping than studies based on data from other regions. This study uhttps://sv.overleaf.com/project/5f5a17fa31656b0001d21002ses both rains and urban catchments customized for Sweden as inputs for the hydraulic modeling.

The study is also probably unique in the respect that it uses raincells with intensities approximated as Gaussian functions as input for hydraulic modelling.

When most earlier studies regarding the subject uses representations of specific catchments in their modelling, this study uses a catchment model designed for representing Swedish urban catchments in general. This enables the results to be fairly applicable to more than one specific city, but at the same time it is not particularly well fitted for any place. Since the aim of this study is not providing exact numbers, but rather obtain general indices on how the size of catchments and raincells affect the hydraulic peak responses, a general model seemed better suited. The generalized design of the urban catchment model with catchments of different sizes, where solely the sizes in practice differentiated the catchments, enabled comparisons between different sizes on equal

terms.

8.4.2 The urban catchment model

The results and conclusion of this study must consider that an idealized catchment model is used, rather than a replica of any specific place. The upsides with this is its general applicability within Swedish cities. At the same time, over generalizing risks giving results not representable anywhere.

The urban model has many model parameters which all influence the hydraulic response. The sensitivity of these parameters has not been tested in simulations. Two of the most important model parameters are topography and proportion of hardened surfaces. A higher proportion of hardened surfaces leads to larger hydraulic peak responses and faster flow processes. A steeper topography also leads to faster flow processes and possibly also larger hydraulic peak responses. The results of the study has shown to be dependent on the size of the peak contribution area, which in turn is dependent on the topography and the proportion of hardened surfaces.

The model topography can be considered representative for most larger cities in Sweden, except those located in hilly terrain with higher relative height differences, like Jönköping and Sundsvall, see Section 6.3. Urban catchments with hilly terrain can expect faster flow processes, and hence a larger peak contribution area.

The proportion of hardened surfaces used in the model - 38 % - is based on a weighted mean value of the runoff coefficients for different types of urban areas, including green structure (Svenskt Vatten, 2004). The runoff coefficient is a measure of the proportion of the precipitation leading to surface runoff, which can be considered corresponding to the proportion of hardened surface. The influence from the ratio of hardened surface on the results of hydraulic peak responses has not been tested in this study. A higher proportion of hardened surfaces will lead to less possible infiltration, and hence higher surface runoff and hydraulic peak responses. Since the proportion of hardened surfaces influences the flow speeds, an increase in the proportion might also lead to a larger peak contribution area. The variability of the amount of hardened surfaces in Sweden could hence risk decreasing the applicability of the results. A catchment with a higher proportion of hardened surfaces, like a city center, might show greater differences between spatially varied and uniform rains, regarding peak response. On the other hand, individual catchments constituted by city centers or other areas with very high proportions of hardened surfaces only, hardly ever get particularly large in Sweden.

The catchments A, B, C and D in the urban model had sizes of 4, 16, 36 and 64 km^2 respectively. This can be compared with the statistics of Swedish urban catchment sizes found by Tusher (2019a), according to the definition in section 2.5, which were regarded relevant for pluvial flooding. More than 95 % of the catchments showed to be smaller than 5 km^2, while the very greatest had a size of 33 km^2 (Tusher, 2019b). The effect of spatially varied rains on the hydraulic responses can be expected to increase with larger catchment sizes. The biggest effect of the spatial rain variation for Swedish urban catchments can hence be expected to be caught by the study. The outlet centered scenarios do not use catchment D, but still cover the size interval of urban catchments in Sweden.

The small differences in hydraulic response between spatially varied Gaussian rains and both types of uniform reference rains for the smallest catchment, show that the spatial variation of rain is of small relevance for most Swedish catchments. Catchments smaller than 4 km^2 can be expected to have even smaller differences in hydraulic responses.

8.4.3 The Gaussian test rains

The Gaussian shaped test rains in this study are based on the assumption that the intensity of individual convective raincells can be approximated as Gaussian functions over space. Several studies have found this to be the case (Sharon, 1972; Zawadski, 1973; Marshall, 1980), and Jinno et al. (1993) uses this assumption in his study. Considering the analysed radar data, a visual inspection can confirm that this seems to be a reasonable assumption for many raincells. In this study, no test has been performed to confirm this quantitatively though, since the rough resolution of the radar data made it not feasible. It is a weakness of the study that the assumption that it is based upon, never is tested. Nevertheless, a Gaussian shape approximation of raincells must be a more skillful description of their spatial distribution than a uniform design rain. The purpose of this study is not to provide exact numbers, but rather to show indices on how the size of raincells and catchment areas affect the hydraulic peak responses. In that context, representation of raincells as Gaussian ellipses can be considered sufficient.

As previously stated in Section 5.4, the radar analysis is encumbered with some uncertainties, even beyond the assumption that the raincells can be approximated as normally distributed. Firstly, the spatial resolution of the radar data (2 km x 2 km) is too rough to describe the spatial resolution of the smaller raincells in a satisfying way. Secondly, the non automated method for deciding the length and width of the raincells which is built on visual inspection, might be seen as slightly subjective.

The derivation of the Gaussian raincell sizes from the radar data is based on the assumption that the relative sizes of raincells is independent of the return period of the rain events, since the relative sizes in the radar analysis is obtained without regard to the maximum accumulated rain volume. The uncertainty associated with the exact radar intensities would have complicated such a regard, which also would have reduced the size of the selection. The radar analysis anyhow indicated a slight increase in relative cell size with the intensity of the raincells. Smaller ARFs corresponds to smaller relative cell sizes. Studies show contradicting results whether ARFs decrease or not with higher return periods (Svensson & Jones, 2010).

The mean reference rains, calculated as spatial averages of the test rains, can be considered as scaled with ARFs based on the Gaussian test rains, hence originally based on the radar analysis. The ARFs obtained by all three test rains showed to lie well within the interval of several earlier studies on ARFs regarding rains with 1 hour duration, summarized by Thorndahl et al. (2019). The difference between 1 and 2 hours, as used here, can be assumed to be relatively slight. This somewhat solidifies the relevance of the test rains as well as the results obtained from the radar analysis.

In this study, simulations have been performed with the test rains centered in the middle of each catchment, as well as at the outlet of each catchment. The major axis of

the Gaussian ellipses have always been directed diagonally through the catchments along their main drainage path. Since the test rains are based on cumulative raincells, they hence represent a raincell which has travelled along the main drainage path diagonally through the catchments. This might have affected the results heavily. Instead placing the Gaussian test rains with their minor axis along the main drainage path, would have resulted in larger differences between test- and reference rains.

In reality, there are an abundance of places within a large catchment where a raincell might strike with its center, moving in any direction. All possible positions and directions might result in different hydraulic responses. It was not feasible within this study to represent all possible scenarios regarding position and moving direction of the raincells, hence a strict selection had to be made. Centering the rains in the outlet while taking the evaluation parameters from the outlet enables the rain from the whole catchment to contribute to the hydraulic response while comparing the response from the cell centers of test rains with the reference rains. Centering the rains in the centre of the catchment along the main drainage path gives the highest average rainfall over the entire catchment and is commonly used for calculating ARF values (Thorndahl et al., 2019). These two positions were deemed sufficient in order to evaluate the difference in hydraulic response between spatially varied and uniform rains.

8.4.4 Comparison of results from mean and maximum reference rain scenarios

A comparison between the results of the two reference rain comparisons is here discussed. Today maximum reference rains are used for urban cloudburst mapping in Sweden, but might reference rains scaled with ARF:s better approximate the hydraulic response to real rains?

To summarize the results, the hydraulic responses of the maximum reference rain showed slightly higher values than the Gaussian test rains, independent of catchment size. The mean reference rains instead showed smaller hydraulic responses than the test rains, with the difference increasing with larger catchment size. This can be interpreted as that a design rain without ARF would overestimate the hydraulic response to most real rains with less than 10 %, no matter the catchment size, while a design rain with ARF would underestimate the hydraulic peak responses. This underestimation seems to be small for catchment A, where the difference is slightly smaller than for the maximum reference rain, and then it increases fast with catchment size. It appears that ARF:s possibly seem to be the better design rain for catchments with sizes up to 4 km^2. For larger catchment, a design rain without ARF seems to better estimate the hydraulic responses.

The reason for this somewhat unexpected result, is that the hydraulic peak response will be determined by the rain that falls within the peak contribution area. If the catchment gets larger than the peak contribution area, the catchment size ceases to matter for the hydraulic peak response. At that point, the ARF is no longer of any use. So, the ARF can be supposed to estimate peak responses well for catchments with sizes close to the peak contribution area, or smaller. For larger catchments than the peak contribution area, the hydraulic responses of the ARF-rain will decrease with catchment size, while the hydraulic responses of spatially varied rains will remain unchanged, and hence be

increasingly underestimated by the ARF-rain. In that case, a design rain without ARF seems to work better. Since the mean reference rains, corresponding to an ARF, are showing hydraulic responses very close to the test rains in catchment A, it is likely that its area is approximately equal to the peak contribution area. This is probably why the mean reference rain works at least as well as the maximum reference rain in estimating the peak responses in catchment A. In the other, larger catchments, the area exceeds the peak contribution area, hence the mean reference rain underestimates the hydraulic responses. Since none of the test rains were small enough to vary substantially within the peak contribution area, the maximum reference rain did not differ much from the test rains in hydraulic response, no matter the catchment size. The principles are in Figure 29 illustrated in a schematic sketch, showing the peak outflows as function of catchment area, for spatially varied as well as uniform rains.

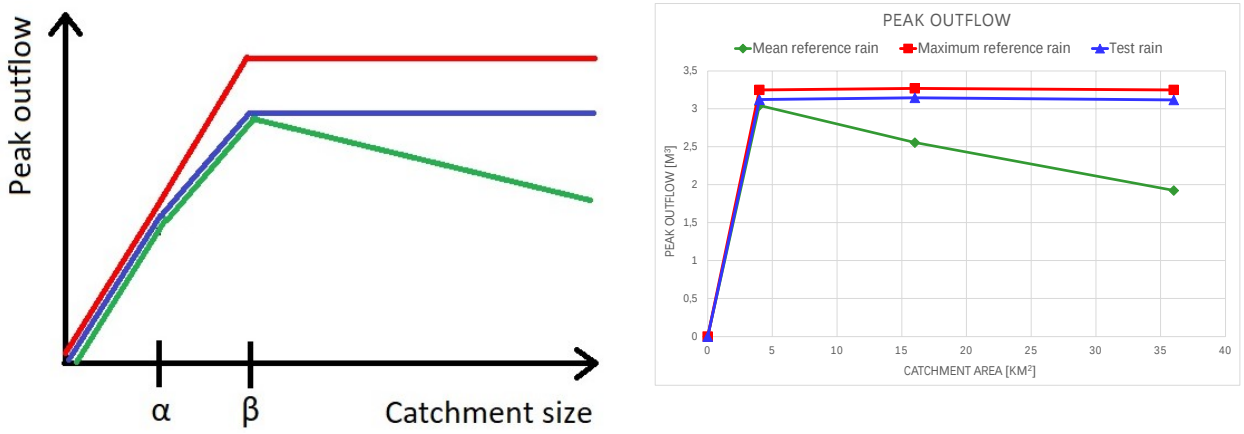

(a) (b)

Figure 28: (a): Schematic sketch showing the theoretical peak outflow plotted against catchment size. The blue line represents a real rain with spatial variation, the red line a uniform design rain without ARF, and the green line a uniform design rain scaled with ARF. α corresponds to the size where the spatial variation of the rain starts to matter, β corresponds to the peak contribution area. If α exceeds β, the spatial variation of the rain will not affect the hydraulic peak responses for any catchment size. (b): The same plot, but with peak outflows obtained from test rain 2 in the study, where the mean reference rain is representing the ARF. A peak outflow of 0 is added at the origin, since an infinitely small area will give an infinitely small outflow. The obtained data seem to correspond well with the theory. The tested catchments are not small enough to describe the increase in peak flow before the peak contribution area is reached, though.

8.4.5 Impact of CDS-hyetographs

The CDS-rain used as hyetograph in this study might be compromising the results. Evaluating the appliance of CDS-rains in Swedish hydraulic design lies outside the scope of this study. However, since the result regarding how the spatial variation of extreme rains affect the hydraulic response might be affected by the temporal aspect of the rain, it is worth discussing how realistic the CDS-rain is in Swedish conditions. The shape of the CDS is extremely pointy. The CDS-rain with 2 hours duration and 100 years return period used in this study has a peak intensity of 176 mm/h. During this peak, 45 % of the total rain volume falls during 10 min, while during 30 min, around two thirds of the total rain volume falls, see Figure 1. This is derived from the intensities corresponding to a 100-year event of the above durations, as the CDS simulates rain of every duration

corresponding to the given return period. This can be considered unrealistic, resulting in a hyetograph with unlikely pointiness. Not only might this lead to overestimation of hydraulic responses, this might also have a decisive role in the magnitude of the difference of hydraulic response between spatially varied and uniform rains. The probably unlikely pointiness of the CDS, where the majority of the rain falls during much less time than two hours, results in an effective duration of the rain - the temporal part of the rain that actually contributes to the hydraulic peak response - much shorter than 2 hours. With a shorter effective rain duration follows a smaller peak contribution area.

A smaller peak contribution area can be expected to lead to smaller differences in hydraulic peak response between test rains and maximum reference rains, since the spatial rain variation within the peak contribution area then will decrease. Hence, using a CDS risks underestimating the difference between spatially varied and uniform rains in hydraulic peak response.

A smaller peak contribution area would instead lead to larger differences in hydraulic peak responses between test rains and spatially uniform reference rains, since the mean rainfall within the peak contribution area then increases for the test rain while it remains unchanged within same area for the mean reference rain. Therefore the CDS might overestimate the difference in hydraulic response between test rains and mean reference rains.

In summary, the unlikely pointiness of the CDS-rain probably underestimates the differences between the hydraulic responses between Gaussian test rains and maximum reference rains, and overestimates the hydraulic responses between Gaussian test rains and mean reference rains. This weakens the conclusion that maximum reference rains better approximate the peak hydraulic response than mean reference rain do, and that there is little need for using ARF:s for Swedish urban catchments. Since the hydraulic responses of test rains obtained in the study are much closer to those of the maximum reference rain than the mean reference rain for catchments larger than catchment A, it is probable that this conclusion still is valid for real rains. Further studies using empirical hyetographs instead of a CDS, would be needed for validating the conclusions.

8.4.6 The rain duration

In this study, only rains with 2 hours duration were tested. For the conclusion that the spatial variation of the rain hardly matters much for the hydraulic peak response to hold for shorter and longer rain durations, it needs to still be true that the accumulated rain does not vary significantly over the peak contribution area. Since the spatial variation of rains decreases with longer duration (Bengtsson & Niemczynowicz, 1986; Dalhström, 2010), this is likely to be true in most cases for all rain durations. Hence, the conclusion of this study can be expected to be representative for other rain durations than the one tested here. Determining this could be a subject for future studies.

8.4.7 Considered parameters

In this study only the peak responses - peak outflows, average maximum water depths and the peak portion of flooded areas - were considered. The duration of the responses is not considered. The duration of the responses will be affected by the spatial variation of the rain over large catchments, since the total amount of runoff is affected of the extent of the

raincells. The larger the rain extent and/or the catchment, the higher the total outflow will be, for example. Even though the peak outflow might not change much, the flow process will then instead be prolonged. Peak responses are often the most important for practical urban implications, but there are exceptions, for example when dimensioning water-retention dams, or considering damage from prolonged standing water. In such cases, the spatial variation of rains might be of high importance.

9 Summary and conclusions

The aim of this study was to obtain improved understanding of how the hydraulic response to extreme rains is affected by the spatial variation of the rain, in order to enable improved cloudburst mapping in Sweden. This was investigated by determining how the hydraulic peak response of an idealized Swedish urban catchment is affected by the spatial variation of extreme rains, in relation to the size of the catchment.

The study showed that a uniform reference rain with the maximum intensity of the Gaussian rain overestimated the hydraulic peak responses with 1-8 %, in comparison with spatially varied Gaussian rains centered at the outlets, independent of the catchment size. The small differences can be interpreted as taking into consideration the spatial variation of rains in cloudburst mapping in Sweden not necessarily being needed.

Uniform reference rains with the mean intensity of Gaussian rains, corresponding to an ARF, underestimated the hydraulic peak responses in comparison with spatially varied Gaussian rains centered at the outlets. The underestimation was less than 5 % for a catchment area of 4 km^2, and thereafter increased with catchment size. In a catchment area of 36 km^2, the peak responses were underestimated with 13-69 %, depending on test rain and evaluation parameter.

The conclusion can be drawn that catchment size ceases to matter for the hydraulic peak response when the time it takes for the whole catchment to contribute to the peak response exceeds the time it takes for the peak to be reached. How much rain varies over the area which is able to contribute to the peak response during the rain event (the peak contribution area), can be assumed to decide how much a design rain without ARF overestimates the peak responses. If the catchment exceeds this size, an ARF-scaled design rain will underestimate the peak responses. This underestimation increases with larger catchments.

The strong temporal pointiness of the CDS-rain used in the study, risks underestimating the difference in hydraulic peak response between the Gaussian rains and the reference rain without ARF, while the difference between test rains and reference rains with ARF risks being overestimated. The study is encumbered with several further uncertainties, for example the orientation of the Gaussian test rains, which risk affecting the results. These can however be assumed to not affect the general conclusion.

Part 3
References and appendices

10 References

Allen, R. J., & DeGaetano, A. T. (2005). Areal reduction factors for two eastern United States regions with high rain-gauge density. Journal of Hydrologic Engineering, 10(4), 327-335.

Arnaud, P., Bouvier, C., Cisneros, L., & Dominguez, R. (2002). Influence of rainfall spatial variability on flood prediction. Journal of Hydrology, 260(1-4), 216-230.

Asquith, W. H., & Famiglietti, J. S. (2000). Precipitation areal-reduction factor estimation using an annual-maxima centered approach. Journal of Hydrology, 230(1-2), 55-69.

Bell, V. A., & Moore, R. J. (2000). The sensitivity of catchment runoff models to rainfall data at different spatial scales. Hydrology and Earth System Sciences, 4(4), 653-667.

Bengtsson, L., & Niemczynowicz, J. (1986). Areal reduction factors from rain movement. Hydrology Research, 17(2), 65-82.

Brath, A., Montanari, A., & Toth, E. (2004). Analysis of the effects of different scenarios of historical data availability on the calibration of a spatially-distributed hydrological model. Journal of Hydrology, 291(3-4), 232-253.

Cole, S. J., & Moore, R. J. (2008). Hydrological modelling using raingauge-and radar-based estimators of areal rainfall. Journal of Hydrology, 358(3-4), 159-181.

Dahlström, B. (2010). Regnintensitet—En Molnfysikalisk Betraktelse. Svenskt Vatten AB: Stockholm, Sweden.

DHI (2017) MIKE 21 - 2D modelling of coast and see. Available from: http://www.mikepoweredbydhi.com/products/mike-21 [2019-01-21].

Dodov, B., & Foufoula-Georgiou, E. (2005). Incorporating the spatio-temporal distribution of rainfall and basin geomorphology into nonlinear analyses of streamflow dynamics. Advances in water resources, 28(7), 711-728.

Durrans, S. R., Julian, L. T., & Yekta, M. (2002). Estimation of depth-area relationships using radar-rainfall data. Journal of hydrologic Engineering, 7(5), 356-367.

Gabellani, S., Boni, G., Ferraris, L., Von Hardenberg, J., & Provenzale, A. (2007). Propagation of uncertainty from rainfall to runoff: A case study with a stochastic rainfall generator. Advances in water resources, 30(10), 2061-2071.

Grebner, D., & Roesch, & Thomas (1997). Regional dependence and application of DAD relationships. IAHS Publication, (246), 223-230.

Grip, H., & Rodhe, A. (1994). Vattnets väg från regn till bäck, 3., rev. upplagan. Stockholm: Hallgren & Fallgren Studieförlag AB.

Hendriks, M. (2010). Introduction to physical hydrology. Oxford University Press.

Hernebring, C., Milotti, S., Steen Kronborg, S., Wolf, T. & Mårtensson, E. (2015). Skyfallet i sydvästra Skåne 2014-08-31. Fokuserat mot konsekvenser och relation till regnstatistik i Malmö. VATTEN: Journal of Water Management and Research, (71), ss. 85–99. Available: https://www.tidskriftenvatten.se/wpcontent/uploads/2017/04/48_article_4764.pdf [2019-02-28].

Jinno, K., Kawamura, A., Berndtsson, R., Larson, M., & Niemczynowicz, J. (1993). Real–rainfall prediction at small space–scales using a two–dimensional stochastic advection–diffusion model. Water Resources Research, 29(5), 1489–1504.

Johansson, B., & Chen, D. (2003). The influence of wind and topography on precipitation distribution in Sweden: Statistical analysis and modelling. International Journal of Climatology: A Journal of the Royal Meteorological Society, 23(12), 1523-1535.

Leijonhufvud, E. (2018). Miljonkostnad för kommunen i skyfallets spår. SVT. https://www.svt.se/nyheter/lokalt/uppsala/miljonkostnad-i-skyfallets-spar [2020-03-02]

Lobligeois, F., Andréassian, V., Perrin, C., Tabary, P., & Loumagne, C. (2014). When does higher spatial resolution rainfall information improve streamflow simulation? An evaluation using 3620 flood events. Hydrology and Earth System Sciences, 18(2), 575-594.

Lyngfelt, S. (1981). Dimensionering av dagvattensystem-rationella metoden. Chalmers University of Technology.

Marshall, R. J. (1980). The estimation and distribution of storm movement and storm structure, using a correlation analysis technique and rain-gauge data. Journal of Hydrology, 48(1-2), 19-39.

Myndigheten för samhälsskydd och beredskap (2017).Vägledning för skyfallskartering : tips för genomförande och exempel på användning. Publikationsnummer:MSB1121 - augusti 2017 ISBN: 978-91-7383-764-4.

Nicótina, L., Alessi Celegon, E., Rinaldo, A., & Marani, M. (2008). On the impact of rainfall patterns on the hydrologic response. Water Resources Research, 44(12).

Olsson, J. (2019). The influence of storm movement and temporal variability of rainfall on urban pluvial flooding: 1D-2D modelling with empirical hyetographs and CDS-rain.

Olsson, J., Simonsson, L., & Ridal, M. (2014). Rainfall nowcasting: Predictability of short-term extremes in Sweden. Urban Water Journal, 11(7), 605-615.

Patil, S. D., Wigington Jr, P. J., Leibowitz, S. G., Sproles, E. A., & Comeleo, R. L. (2014). How does spatial variability of climate affect catchment streamflow predictions?. Journal of hydrology, 517, 135-145.

Pechlivanidis, I. G., McIntyre, N., & Wheater, H. S. (2017). The significance of spatial variability of rainfall on simulated runoff: an evaluation based on the Upper Lee catchment, UK. Hydrology Research, 48(4), 1118-1130.

Raab, B., & Vedin, H. (Eds.). (1995). Sveriges Nationalatlas: klimat, sjöar och vattendrag. Bra böcker.

SHARON, D. (1972). Spatial analysis of rainfall data from dense networks. Hydrological Sciences Journal, 17(3), 291-300.

Singh, V. P. (1997). Effect of spatial and temporal variability in rainfall and watershed characteristics on stream flow hydrograph. Hydrological processes, 11(12), 1649-1669.

Skaugen, T. (1997). Classification of rainfall into small-and large-scale events by statistical pattern recognition. Journal of Hydrology, 200(1-4), 40-57.

SMHI (2020). Extrem punktnederbörd.https://www.smhi.se\kunskapsbanken\meteorologi\extrem–punktnederbord–1.23041 [2020-09-21]

SMHI (2019). Nyckfulla sommarskurar . https://www.smhi.se/kunskapsbanken/nyckfulla-sommarskurar-1.17129 [2020-09-27]

SMHI (2018). Extrem nederbörd. https://www.smhi.se/kunskapsbanken/meteorologi/extrem-nederbord-1.23060 [2020-09-20]

SMHI (2017). Skyfall och rotblöta. https://www.smhi.se/kunskapsbanken/rotblota-1.17339 [2021-09-15]
Smith, M. B., Koren, V., Zhang, Z., Zhang, Y., Reed, S. M., Cui, Z., ... & Anderson, E. A. (2012). Results of the DMIP 2 Oklahoma experiments. Journal of hydrology, 418, 17-48.

Svenskt vatten (2011). Nederbördsdata vid dimensionering och analys av avloppssystem. P104

Svenskt vatten (2004). Dimensionering av allmänna avloppsledningar. P90

Svensson, C., & Jones, D. A. (2010). Review of methods for deriving areal reduction factors. Journal of Flood Risk Management, 3(3), 232-245.

Syed, K. H., Goodrich, D. C., Myers, D. E., & Sorooshian, S. (2003). Spatial characteristics of thunderstorm rainfall fields and their relation to runoff. Journal of Hydrology, 271(1-4), 1-21.

Thorndahl, S., Nielsen, J. E., & Rasmussen, M. R. (2019). Estimation of Storm-Centred Areal Reduction Factors from Radar Rainfall for Design in Urban Hydrology. Water, 11(6), 1120.

Tusher, M. D. A. (2019a). Impact of Extreme Rainfall Event over Swedish Urban Catchments: A study on catchment characterization in the context of Aerial Reduction Factor and storm movement.
Retrieved from http://urn.kb.se/resolve?urn=urn:nbn:se:kth:diva-266469

Tusher, M. D. A. (2019b). Impact of Extreme Rainfall Event over Swedish Urban Catchments: A study on catchment characterization in the context of Aerial Reduction Factor and storm movement. [unpublished material, personal communication].

United States Department of Agriculture (1986). Urban Hydrology for Small Watersheds TR-55. Technical Release 55.

Watt, E., & Marsalek, J. (2013). Critical review of the evolution of the design storm event concept. Canadian Journal of Civil Engineering, 40(2), 105-113.

Zawadzki, I. I. (1973). Statistical properties of precipitation patterns. Journal of Applied Meteorology and Climatology, 12(3), 459-472.

11 Appendices

11.1 Appendix A Results of test rains compared with maximum reference rains with areal evaluation parameters

In Table 17-19, the average maximum water depth and proportion area flooded with at least 0.1 m water during some time of the simulation, is shown for the spatially varied Gaussian test rains.

Table 13: Hydraulic responses for area centric simulations with Test rain 1.

Catchment area	**Average maximum water depth** [m]	**Proportion flooded area** [%]
A (4 km^2)	0.0447	8.19
B (16 km^2)	0.0373	5.85
C (36 km^2)	0.0287	3.66
D (64 km^2)	0.0217	2.31

Table 14: Hydraulic responses for area centric simulations with Test rain 2.

Catchment area	**Average maximum water depth** [m]	**Proportion flooded area** [%]
B (16 km^2)	0.0418	7.08
C (36 km^2)	0.0357	5.20
D (64 km^2)	0.0294	3.63

Table 15: Hydraulic responses for area centric simulations with Test rain 3.

Catchment area	**Average maximum water depth** [m]	**Proportion flooded area** [%]
A (4 km^2)	0.0471	8.81
B (16 km^2)	0.0450	8.09
C (36 km^2)	0.0414	6.81
D (64 km^2)	0.0373	5.45

In Tables 22-24 below, the hydraulic responses of the Gaussian test rains are normalized by dividing with the responses of the maximum reference rain. The spatial average rain amount over the areas is also shown, as a proportion of the maximum reference rain of 62.5 mm, and hence normalized in accordance with the other shown parameters.

Table 16: Normalized hydraulic responses for **test rain 1** centered in the middle of respective catchment area

Catchment area	**Average rain volume**	**Average maximum water depth**	**Proportion flooded area**
A (4 km^2)	0.95	0.93	0.90
B (16 km^2)	0.83	0.78	0.64
C (36 km^2)	0.67	0.60	0.39
D (64 km^2)	0.53	0.45	0.23

Table 17: Normalized hydraulic responses for **test rain 2** centered in the middle of respective catchment area.

Catchment area	**Average rain volume**	**Average maximum water depth**	**Proportion flooded area**
A (4 km^2)	0.97	0.96	0.94
B (16 km^2)	0.90	0.87	0.77
C (36 km^2)	0.78	0.74	0.56
D (64 km^2)	0.68	0.61	0.39

Table 18: Normalized hydraulic responses for **test rain 3** centered in the middle of respective catchment area

Catchment area	**Average rain volume**	**Average maximum water depth**	**Proportion flooded area**
A (4 km^2)	0.99	0.98	0.97
B (16 km^2)	0.95	0.94	0.88
C (36 km^2)	0.89	0.86	0.73
D (64 km^2)	0.82	0.77	0.53

Table 19: Hydraulic responses for **test rain 1**, centered around the outlet of respective catchment area. Average maximum water depth and proportion flooded area applies for a square area of 500 m x 500 m closest upstream the outlet of respective catchment area

Catchment area	**Peak outflow** $[m^3/s]$	**Average maximum water depth** [m]	**Proportion flooded area** [%]
A (4 km^2)	3.02	0.066	24.5
B (16 km^2)	3.05	0.066	24.9
C (36 km^2)	3.02	0.066	24.5

Table 20: Hydraulic responses for **test rain 2**, centered around the outlet of respective catchment area. Average maximum water depth and proportion flooded area applies for a square area of 500 m x 500 m closest upstream the outlet of respective catchment area

Catchment area	**Peak outflow** $[m^3/s]$	**Average maximum water depth** [m]	**Proportion flooded area** [%]
A (4 km^2)	3.12	0.067	24.6
B (16 km^2)	3.15	0.067	25.1
C (36 km^2)	3.12	0.067	24.6

Table 21: Hydraulic responses for **test rain 3**, centered around the outlet of respective catchment area. Average maximum water depth and proportion flooded area applies for a square area of 500 m x 500 m closest upstream the outlet of respective catchment area

Catchment area	**Peak outflow** $[m^3/s]$	**Average maximum water depth** [m]	**Proportion flooded area** [%]
A (4 km^2)	3.19	0.069	25.5
B (16 km^2)	3.21	0.069	25.9
C (36 km^2)	3.19	0.069	25.9

In Tables 25-27 below, the hydraulic responses of the test rain are normalized by dividing with the responses of the maximum reference rain for respective catchment area.

Table 22: Normalized hydraulic responses for **test rain 1**, centered around the catchment outlet.

Catchment area	**Peak outflow**	**Average maximum water depth**	**Proportion flooded area**
A (4 km^2)	0.930	0.945	0.934
B (16 km^2)	0.931	0.951	0.954
C (36 km^2)	0.931	0.948	0.943

Table 23: Normalized hydraulic responses for **test rain 2**, centered around the catchment outlet.

Catchment area	**Peak outflow**	**Average maximum water depth**	**Proportion flooded area**
A (4 km^2)	0.960	0.958	0.945
B (16 km^2)	0.962	0.959	0.960
C (36 km^2)	0.961	0.958	0.947

Table 24: Normalized hydraulic responses for **test rain 1**, centered around the catchment outlet.

Catchment area	**Peak outflow**	**Average maximum water depth**	**Proportion flooded area**
A (4 km^2)	0.981	0.986	0.978
B (16 km^2)	0.982	0.987	0.992
C (36 km^2)	0.982	0.987	0.978

11.2 Appendix B Results of test rains compared with mean reference rains with areal evaluation parameters

In Table 24, the spread ratio of both average maximum water depth and proportion flooded area are shown.

Table 25: The evaluation parameter spread ratio calculated from both mean maximum flooding depth and proportion flooded area, extracted from the result files of the test rain and mean reference rain simulations for each rain+catchment combination.

Test rain and catchment	**Spread ratio of average maximum water depth**	**Spread ratio of proportion flooded area**
test1-A	1.16	1.23
test1-B	2.86	15.5
test1-C	9.19	386
test1-D	15.7	Infinity
test2-A	1.1	1.16
test2-B	1.67	2.97
test2-C	4.07	26.17
test2-D	9.80	Infinity
test3-A	1.05	1.09
test3-B	1.14	1.51
test3-C	1.99	3.30
test3-D	3.28	26.12

Table 14, 15 and 16 show the normalized hudraulic peak responses of for test rain 1, test rain 2 and test rain 3 on catchment A, B and C are shown.

Table 26: Normalized hydraulic peak responses for **test rain 1**, centered around the catchment outlet.

Catchment area	**Peak outflow**	**Average maximum water depth**	**Proportion flooded area**
A (4 km^2)	1.04	1.04	1.05
B (16 km^2)	1.31	1.50	1.48
C (36 km^2)	1.79	3.21	2.36

Table 27: Normalized hydraulic peak responses for **test rain 2**, centered around the catchment outlet.

Catchment area	**Peak outflow**	**Average maximum water depth**	**Proportion flooded area**
A (4 km^2)	1.01	1.01	1.03
B (16 km^2)	1.15	1.19	1.23
C (36 km^2)	1.39	1.63	1.62

Table 28: Normalized hydraulic peak responses for **test rain 3**, centered around the catchment outlet.

Catchment area	**Peak outflow**	**Average maximum water depth**	**Proportion flooded area**
A (4 km^2)	1.02	1.03	1.01
B (16 km^2)	1.08	1.09	1.10
C (36 km^2)	1.17	1.15	1.28